crystals

MDPI

Article

Semiquantitative X-ray Powder Diffraction Analysis in Counterfeit Medicines Investigation—The Viagra Example

Armand Budzianowski [1,*], Karolina Pioruńska-Sędłak [2], Magdalena Popławska [2], Jan K. Maurin [2] and Agata Błażewicz [2,*]

[1] National Centre for Nuclear Research, Andrzeja Sołtana 7, 05-400 Otwock, Poland
[2] National Medicines Institute, Chełmska 30/34, 00-725 Warsaw, Poland; k.piorunska@nil.gov.pl (K.P.-S.); m.poplawska@nil.gov.pl (M.P.); j.maurin@nil.gov.pl (J.K.M.)
* Correspondence: armand.budzianowski@ncbj.gov.pl (A.B.); a.blazewicz@nil.gov.pl (A.B.)

Abstract: Have you ever looked at a powder diffractogram during a routine qualitative test and wondered how much of a particular powder compound is in the powder material? Several methods can work this out, but none of them could be used in our case because something was missing from each in performing a rapid quantity test for an active ingredient in a tablet. A semiquantitative method of an X-ray powder diffraction analysis of products containing sildenafil citrate is proposed. This method utilizes calibration curves for the most common compositions encountered in falsified and not-registered Viagra analogues. Sildenafil doses are established for singularly prepared powder probes of a medicinal product, and two runs of data collection are used: the first, the fast one, for the qualitative analysis of the product, and the second for selected 2θ regions for the API and identified excipients. An example of a product composed mainly of sildenafil citrate, gypsum and microcrystalline cellulose is discussed in detail. The data obtained from X-ray experiments were compared with the results obtained from validated liquid chromatography coupled to a diode array detector and mass spectrometry methods.

Keywords: Viagra; sildenafil; X-ray powder diffraction; XRPD; semiquantitative analysis; falsified medicines

Citation: Budzianowski, A.; Pioruńska-Sędłak, K.; Popławska, M.; Maurin, J.K.; Błażewicz, A. Semiquantitative X-ray Powder Diffraction Analysis in Counterfeit Medicines Investigation—The Viagra Example. *Crystals* **2023**, *13*, 1485. https://doi.org/10.3390/cryst13101485

Academic Editor: Sławomir Grabowski

Received: 31 August 2023
Revised: 3 October 2023
Accepted: 4 October 2023
Published: 12 October 2023

1. Introduction

The turn of the century brought an expansion of the counterfeiting of medicines, or at least the consciousness of the problem [1,2]. Several "epidemic diseases" in developing countries had been related to falsified or low-quality medicines. As an example, the observation of fatal renal problems in children in Bangladesh, which were caused by the presence of ethylene glycol in paracetamol elixir [3]. Similarly, many deaths due to malaria in Southeast Asia had been related to falsified artesunate [4–6]. In broad terms, the WHO defines falsified medical products to be those that are deliberately/fraudulently misrepresented with respect to their identity, composition or source. This includes the substitution, adulteration or reproduction of an authorized medical product or the manufacture of a medical product that is not an authorized product [7–9], [10] (pp. 195, 197, 243).

At least nine types of falsification can be distinguished [10,11], the first being products that contain the same active pharmaceutical ingredient (API) and excipients as the original medicine, are correctly packaged and labelled but are illegally imported and distributed. Other types of falsification are products that have the original packaging, and contain the same ingredients as the genuine medicine but contain incorrect amounts of ingredients. Another type of falsification comprises products that, despite being identical from an external point of view and having genuine packaging, contain no active ingredients. There are also products that, despite being identical from an external point of view and having similar packaging, contain different excipients than the original medicine. Outwardly, these products look similar to the original in their genuine packaging but contain different

or harmful substances instead of the declared active ingredients. The next category is known products with counterfeit packaging and the correct amounts of active ingredients. There are also products with counterfeit packaging but with different amounts of active ingredients. Others are products with counterfeit packaging that contain a different active ingredient. Finally, there are products with counterfeit packaging that do not contain active ingredients. These categories, all being intellectual property rights offences, are of different importance from the patient's health point of view. Hence, the external view and the packaging are less important than the product composition, and then the excipient content (if neutral) is less important than the active ingredient content, and finally, a lower dose is less harmful (especially in the case of the title Viagra) than a higher dose.

According to the WHO, in a period from 2013 to 2017, the main categories of substandard and falsified products were anti-malarial (19.6%), antibiotics (16.9%), anesthetics and painkillers (8.5%), lifestyle products (8.5%), cancer medicines (6.8%) and others (39.7%) [12] (p. 12), [13].

Although there are not many known serious problems with pharmaceutical products containing phosphodiesterase type-V inhibitors, they are the most frequently falsified medicinal products encountered in Europe and in other developed countries of the world. As far as this applies to all products from this group, the most frequently falsified product is Viagra from Pfizer, and therefore, our attention was mainly aimed at this product as an example in the group. Our experience, as well as data reported by Pfizer [14], show that the majority of counterfeit Viagra tablets contain no API (24%) or a lower dose of the active ingredient (57%), and only rarely a higher dose of it (9%). Another issue is the possible risk connected with substandard medicines [15]. This is very often connected with the low quality of active ingredients, which was shown lately by Keizers et al. for sildenafil found in falsified erectile dysfunction products [16]. In recent years, we have studied many samples of Viagra using X-ray powder diffraction (XRPD). We showed previously that this method could be used as a very convenient "fingerprint" method, enabling distinguishing between original and falsified products even by non-professionals [17]. The XRPD method is, however, a very powerful method of qualitative analysis. In the case of falsified products, it could be used to identify not only active ingredients but also different excipients, including those not declared by the manufacturer of the original product, which is sometimes hard to identify using standard high-performance liquid chromatography (HPLC) or spectroscopic methods. One of the very important issues that could be solved by X-ray diffraction is the problem of distinguishing between polymorphic forms or different solvates of a given chemical substance. Such forms differ from each other significantly in their powder diffraction patterns, which we have also demonstrated previously for Acomplia samples [18].

Analytical Methods Used in Counterfeit/Falsified Medicines Investigations

Several physicochemical methods have been employed lately to distinguish falsified products from original medicinal products. The methods range from very simple, e.g., thin-layer chromatography [19], proposed for movable field laboratories, to more expensive and sophisticated methods based on near-infrared (NIR) or Raman spectroscopy [20], utilized in equipment used by customs and border police for drug enforcement purposes to laboratory methods used both in qualitative and quantitative analyses. Some methods, such as NIR, were demonstrated to be suitable as characteristic fingerprints (even without sample preparation) and can be used in cluster analyses in combination with chemometric methods [21]. Other methods, e.g., XRPD, as we tried to show some years ago for Viagra [18], can be used as fingerprints of the product even without any mathematical or statistical treatment. Importantly, some of the methods such as NIR, XRPD or Raman spectroscopy are non-destructive methods and can be used not only as fingerprinting but also as qualitative methods. Many spectroscopic methods give spectra characteristics not only for APIs but also for crystalline excipients [22]. It was demonstrated for instance that the Raman method gives characteristic spectra for both API and almost all excipients

declared in original Viagra [23]; but, as shown there, the Raman spectra of sildenafil citrate and the finished product are very similar and not discernible for non-professionals. The same applies to Fourier-transform infrared spectroscopy (FTIR) when using the attenuated total reflectance (ATR) method. Both Raman and FTIR spectrometers can be relatively small and in the case of Raman even hand-held. It is different in the case of X-ray diffractometers which are, even in the smallest benchtop version, much bigger and more expensive than the former. Contrary to other methods, however, XRPD is a method of choice for all crystalline materials, especially for inorganic or mineral substances which give very sharp and characteristic diffraction patterns.

Mass spectrometry (MS) coupled to liquid chromatography (LC) is very useful in falsified medicines analysis. The use of a time-of-flight (TOF) analyzer is helpful, as it allows accurate mass measurements, and hence the assessment of empirical formulas of unknown analogues of API [24]. Using only MS spectra to identify unknown substances is not sufficient, as different substances could have the same empirical formula but different fragmentation patterns; therefore, using quadrupole and MS/MS mode is obligatory. The advantages of LC–QTOF-MS include its high specificity, sensitivity and ability to identify unknown substances. The QTOF-MS/MS uniquely offers three dimensions of identification information simultaneously on all results: precise mass, isotopic pattern and MS/MS fragmentation pattern.

2. Materials and Methods

2.1. Standards and Reagents

2.1.1. XRPD

Sildenafil citrate from a not-registered manufacturer secured by border police was applied in X-ray studies as the working standard. The quality of this chemical was checked using XRPD and HPLC techniques comparing it with the sildenafil citrate standard from Polpharma (Starogard Gdański, Poland).

Calcium hydrogen phosphate dihydrate ($CaHPO_4 \cdot 2H_2O$), calcium carbonate ($CaCO_3$) and calcium sulphate hemihydrate ($CaSO_4 \cdot 0.5H_2O$) were from Chempur(Piekary Śląskie, Poland); cellulose (microcrystalline) and corn starch were from Sigma Aldrich, (Saint Louis, MO, USA), whereas lactose hydrate was from POCH, (Gliwice, Poland).

Calcium sulphate hemihydrate comprised a mixture of two phases, calcium sulphate (anhydrite $CaSO_4$) and calcium sulphate dihydrate (gypsum $CaSO_4 \cdot 2H_2O$). Hence, we cannot use bassanite (calcium sulphate hemihydrate) in constructing calibration curves. Therefore, we decided to use gypsum instead. Gypsum is a soft crystalline mineral. To be sure to have a pure polymorphic form, we decided to use a large monocrystal (from a natural source). We micronized the gypsum sample in an agate mortar. The powder was sieved through the sieve and then analyzed by XRPD. The analysis confirmed the single-phase form of calcium sulphate dihydrate.

Appendices A and B (Tables A1 and A2) provide additional numerical information, such as the mass absorption coefficients of the substances used.

2.1.2. LC-DAD, LC-QTOF-MS

Methanol purchased from Merck Millipore (LiChrosolv; Darmstadt, Germany), acetonitrile from AppliChem (Maryland Heights, MO, USA) and formic acid from Fluka (a subsidiary of Merck Millipore), all of LC-MS grade, and doubly distilled water additionally purified in the Nanopure Diamond UV Deionization System from Barnstead (a part of Thermo Fisher Scientific, Waltham, MA, USA) were used throughout. Sildenafil citrate was supplied by Polpharma.

2.2. Samples

Three control samples C01, C02 and C03 of known concentration and two real falsified samples, denoted F01 and F02, of unknown compositions were analyzed. Many real falsified samples were submitted by the police to our laboratory for testing; however, only

F01 and F02 samples were selected because they contained sildenafil citrate, gypsum and microcrystalline cellulose. The composition was confirmed by the XRPD technique. Both samples consisted of pale blue (F01) or blue (F02) rounded-diamond-shape film-coated tablets with "Pfizer" imprinted on one side and "VGR100" on the other side. The imprints suggested a declared dose of 100 mg of sildenafil.

The samples C01, C02 and C03 were prepared in our laboratory and contained only sildenafil citrate, calcium sulphate dihydrate and microcrystalline cellulose. The concentrations of C01 were 74.6 mg (16.14%) + 22.7 mg (4.91%) + 365.0 mg (78.95%), respectively. The total weight of the sample was 462.3 mg. The concentrations of C02 were 45.0 mg (8.32%) + 141.3 mg (26.13%) + 354.5 mg (65.55%), respectively, and the total weight was 540.8 mg. The concentrations of C03 were 87.2 mg (20.31%) + 114.6 mg (26.69%) + 227.5 mg (52.99%), respectively, and the total weight was 429.3 mg.

2.3. XRPD Analysis

The availability of standard samples or calibration coefficients and the frequency of analysis determine the choice of a quantitative or semi-quantitative XRD method. If the analyte is pure, the single or dual line addition model applies, but it results in the contamination of samples. The reference intensity ratio (RIR) method can be used for all reflections or can be limited to a few reflections for mixtures where all phases can be detected. This method is not applicable here due to some identification problems, the lack of references in the database or the lack of structural information. The Rietveld method involves the use of crystallographic structures and calculates powder diffractograms for initial parameters that describe an instrument. Finally, the curves of all phases are summed, the background is added, and sometimes curves calculated by the LeBail or the Pawley methods are added. The result is compared with the experimental measurement. The ratio of each phase can then be adjusted to obtain the best fit for the experimental data. This allows the phase ratio to be determined. Apart from the disadvantage of refinement of crystal structures from powder data, it also requires the knowledge of the crystal structure of each of the phases. The presence of an amorphous phase makes this task even more difficult.

Well-known calibration line methods apply for the straight line with the correlation $C_i = f(I_i)$ such as the general model, the straight line calibration model, the internal standard model and the matrix flushing model. The linear regression method applies to different substances with similar absorption coefficients. The correlation equation $C_i = f(I_i)$ presented below is more general and can be useful when the absorbance of all samples is not the same and for a nonlinear calibration curve. It is intended to be an easy-to-use method for semi-quantitative X-ray powder diffraction analysis. A visualization of the steps and performed decisions to convert intensity into estimated concentration [%] and/or mass [mg] is shown in Figure 1. To simplify the illustration, the procedures for repeating the intensity determination of reflections with different backgrounds around a reflection to obtain more data and calculate arithmetic averages have been omitted.

2.3.1. Instrumentation

X-ray powder diffraction was carried out using a Bruker D8 Advance diffractometer. The Bragg–Brentano configuration with a θ-θ goniometer was used with a 1D position-sensitive detector Våntec. The CuK_α monochromatic radiation was applied. For qualitative analyses (denoted QA), the applied 2θ range was usually between 5° and 60° and a step size of 0.021° or sometimes smaller (0.014° or 0.007°) was used. However, for quantitative analyses, a step size of 0.014° or sometimes 0.007° was used (denoted S-QTY). The 2θ range depends on the sample, e.g., for sildenafil citrate the 2θ range between 6.6° and 11° was used.

The best ratio between a step size and a measurement time per step was chosen to obtain optimal parameters and measurement times as short as possible. All diffractogram interpretations were performed using EVA software from Bruker AXS [25] and powder

diffraction databases. Samples were prepared at 298 K and mounted in PMMA specimen holders with a 25 mm diameter and a depth of ~0.7 mm.

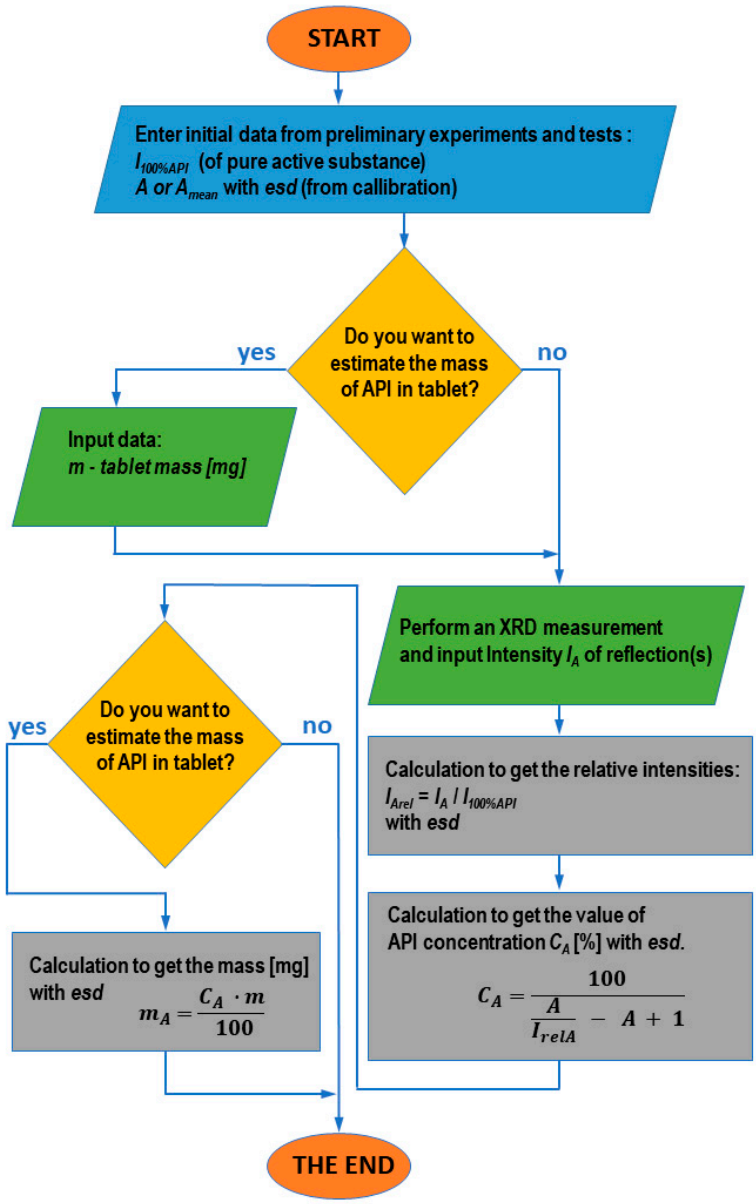

Figure 1. Graphical representation of the algorithm for semi-quantitative X-ray powder diffraction analysis.

2.3.2. Determination of Intensity

For intensities calculation, the EVA software from Bruker [25] was used. However, because some reflections might overlap, the "FPM Model" or "FPM Evaluation" tools were applied. As an alternative method to perform deconvolution of reflections, the TOPAS software from Bruker [26] or a non-commercial alternative, e.g., the Fityk software [27] can be used.

2.3.3. Calibration Curves

Intensities for calibration curves were determined several times for the same diffraction pattern using EVA V14. Different approaches were tested. Reproducible and similar results from various techniques were obtained when a Fourier transform and manual background determination were used. The calibration curves for reflections located in different positions from the 2θ range up to ca. 30° can be significantly different. This is because of various

illuminations of the sample in the Bragg–Brentano configuration and because of Lorentz–polarization correction [28]. Determination of the sulphate concentration may allow for assessment of the absorption of the mixture, which may be a better approach to estimating the concentration of sildenafil in the sample. We describe a methodology using an example of a sample containing sildenafil citrate, calcium sulphate dihydrate and microcrystalline cellulose, which is usually amorphous. There are four possible combinations of two-phase calibration curves: two combinations for sildenafil citrate (i) in calcium sulphate dihydrate and (ii) in microcrystalline cellulose; and two combinations for calcium sulphate dihydrate (iii) in sildenafil citrate and another (iv) in microcrystalline cellulose. Calibration curves were prepared based on reference mixtures with the compositions mentioned above (see Figure 2, Figures A1–A6 in Appendix C, Figure A9 in Appendix F).

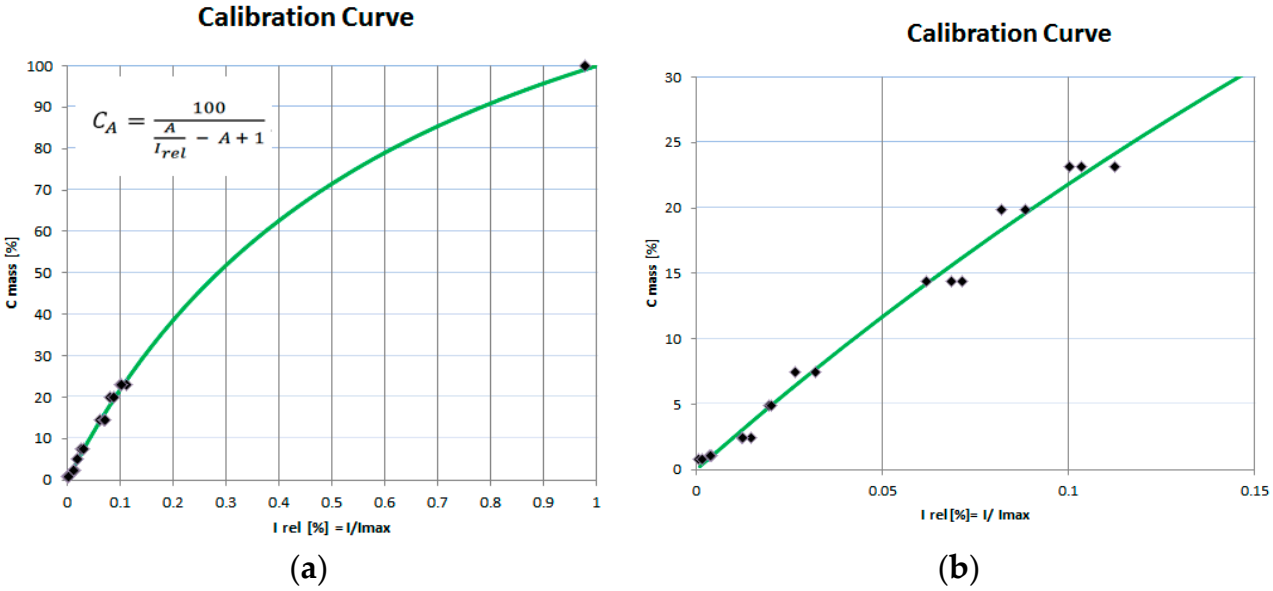

Figure 2. An exemplary calibration curve for two-phase samples containing sildenafil citrate in gypsum (i): (**a**) full range, (**b**) focus on the expected quantity of sildenafil in drugs. The curve has been calculated on the base of the intensities I_2 for a peak at 2θ ~ 8°, which stands for layer (1 0 2) and a systematic absence of reflections (0 1 0) and (2 0 1).

On the calibration curves (e.g., Figure 2a), we have omitted the ranges between low concentrations of sildenafil and 100% because we expect only low concentrations of the active ingredient in falsified products. This can be seen as a mistake, but it is intentional. Higher concentrations are more harmful to humans and should be detectable even if there are no points on the curve.

2.3.4. The Choice of Reflections—Selection of Measurements Ranges

The most crucial issue in the good performance of quantitative analysis is the proper choice of reflections, the intensities of which will be used in further calculations. The possible choices of characteristic reflections for sildenafil citrate and calcium sulphate dihydrate are presented in Figure 3. For sildenafil citrate in calcium sulphate dihydrate (i), three reflections at 2θ ≈ 7.22°, 8.2° or 10.2° could be used. For sildenafil citrate in microcrystalline cellulose (ii), three reflections at 2θ ≈ 7.2°, 8.2° or 10.2° could also be used.

For calcium sulphate dihydrate in sildenafil citrate (iii), more reflections could be used, e.g., at 2θ ≈ 11.6° or 33.3°. However, the reflection at 2θ ≈ 11.6° is overlapping with the very weak reflection from sildenafil citrate at 2θ ≈ 11.4°. The reflection at 2θ ≈ 23.3° is overlapping with the very weak reflection from sildenafil citrate. The reflection at 29° is localized between two reflections at 28.8° and 29.3° from sildenafil citrate—these are hard to separate.

Similarly, many reflections, e.g., at 11.6° or 33.3°, could be used for calcium sulphate dihydrate in microcrystalline cellulose (iv). The reflection at 23.3° is on the slope of a broad amorphous profile of microcrystalline cellulose, but both can be deconvoluted.

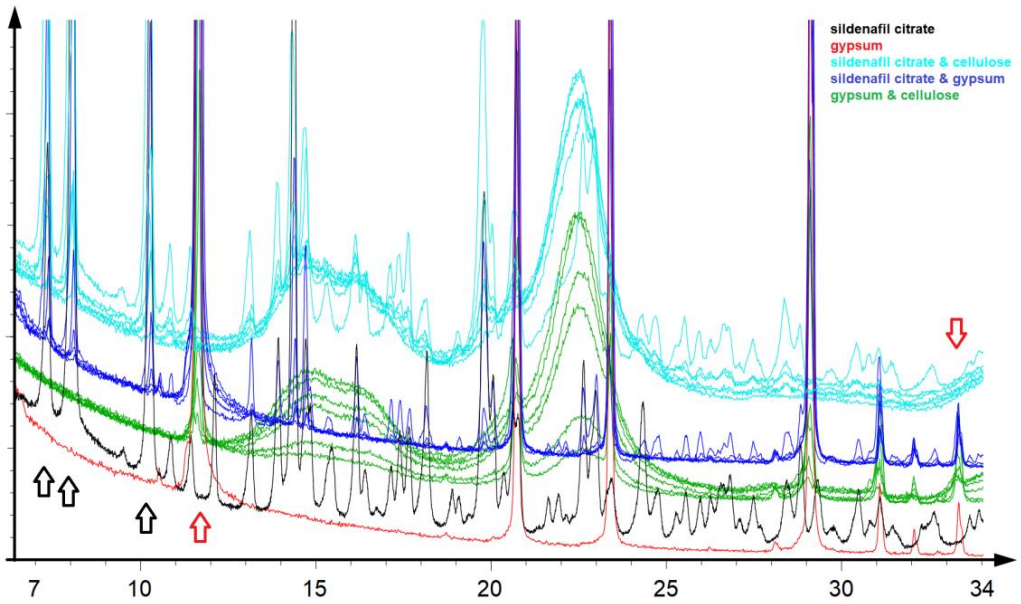

Figure 3. Superimposed XRPD patterns of three exemplary compounds: Sildenafil citrate (black), gypsum (red) and cellulose. The trends in the shape of reflections of these three compounds in the mixed system are shown by including two-phase diffractograms with different percentage compositions. Diffractograms of sildenafil citrate in cellulose in the range of 1–70% are light blue, sildenafil citrate in gypsum in the range of 1–70% is blue and gypsum in cellulose in the range of 1–50% is green. To make the positions of the reflections more visible, the diffractograms are shifted along the intensity axis. The arrows indicate reflections which were selected to perform exemplary XRPD quantity estimations. Black arrows indicate reflections of sildenafil citrate, and the red arrows indicate reflections of the gypsum selected for calibration curves denoted in the text as (i), (ii), (iii) and (iv).

2.4. LC-DAD and LC-QTOF-MS Analysis

2.4.1. Instrumentation and Conditions

A tandem mass spectrometer micrOTOF-QII from Bruker Daltonik (Bremen, Germany) with a time-of-flight analyzer (TOF) coupled to a high-performance liquid chromatography (HPLC) Ultimate 3000 system (Thermo Scientific, Dreieich, Germany) was used. The MS conditions were as follows: ESI positive ion mode, dry gas flow rate 8.0 L·min^{-1}, dry heater 180 °C, capillary voltage 4500 V, end plate offset −500 V, MS data full scan mode (from *m/z* 50 to 1500). A C18 analytical column (Hypersil GOLD, 100 mm × 2.1 mm; 3 µm particle size; Thermo Fisher Scientific, Waltham, MA, USA) with a guard column (Hypersil GOLD, 10 mm × 2.1 mm; 3 µm; Thermo Fisher Scientific) was used. The linear gradient elution at a flow rate of 0.15 mL·min^{-1} was performed using 0.1% formic acid in solvent A (water/acetonitrile 9:1, *v:v*) and 0.1% formic acid in solvent B (methanol/acetonitrile 9:1, *v:v*). After 2 min in initial conditions (10% B), the gradient increased to 90% B in 5 min, with a hold time of 3 min, followed by a linear return to 10% B within 2 min and 2 min stabilization. The diode-array detection (DAD) was set from 190 to 320 nm. A wavelength of 256 nm was chosen for quantification.

2.4.2. Standard Solutions and Matrix Solution

Sildenafil citrate was dissolved in a 1:1:1 (*v/v/v*) mixture of methanol, acetonitrile and water. Stock solutions were prepared at a concentration range from 0.08 to 20 µg·mL^{-1}. Working solutions were prepared by successively diluting stock solutions. The matrix

solution was composed of an 80 mg 1:3 (*w/w*) mixture of calcium sulphate dihydrate and microcrystalline cellulose dissolved in the same solution as standards.

2.4.3. Sample Preparation

Tablets were weighed, powdered and homogenized. Accurately weighed portions of the powder, equivalent to 10 mg or 50 mg of sildenafil, were dissolved with a 1:1:1 (*v/v/v*) mixture of methanol, acetonitrile and water and sonicated. The extracts were further diluted to an appropriate concentration.

2.4.4. Methods Validation

The validity of the method was investigated based on ICH guidelines [29]. Relative standard deviation (RSD) of sildenafil peak retention time and mass errors were investigated to confirm specificity. Additionally, matrix solution chromatograms were investigated, to check for any interfering peaks. Seven concentration levels from 0.08 $\mu g \cdot mL^{-1}$ to 20 $\mu g \cdot mL^{-1}$ were analyzed to estimate a linearity range, and the coefficient of determination (r^2) was calculated. Intra-day and inter-day precision and accuracy were assessed at three concentration levels. Inter-day precision was calculated on three days. RSD value was used for precision evaluation and accuracy was expressed in percentage. A concentration range for which a suitable precision, accuracy and linearity of analytical signals is guaranteed was evaluated.

3. Results

3.1. Qualitative Analysis of Viagra by X-ray Powder Diffraction

X-ray powder diffraction is a very powerful method for the qualitative analysis of all types of crystalline solids. As far as all crystalline components of a sample give increments to the total diffraction pattern, they could also be identified by applying data collected in spacious databases including those that are commercially available [30], open-access [31–34] and user-composed. Using only the Viagra 100 mg example, we can show several analyses where we identified different not-declared excipients or even different APIs.

In Figure 4, examples of the analysis of different alleged Viagra 100 mg tables are presented. Figure 4a represents an original tablet from Pfizer. Microcrystalline cellulose (shown as a dark purple, partially amorphous profile), anhydrous calcium hydrogen phosphate (depicted as vertical pale-blue lines) and sildenafil citrate (shown as vertical red lines) are the three main ingredients. All but the third (Figure 4c) example represent cases where sildenafil was identified—the red vertical lines in Figure 4a,b,d,e correspond to sildenafil citrate, whereas the green vertical lines in Figure 4f could be ascribed to sildenafil in the form of a base. The only example, presented here, which did not contain sildenafil as an API is the case from Figure 4c, where acetaminophen (paracetamol) was identified—depicted as orange vertical lines. Comparing the overall view of the presented diffraction patterns, one can conclude however that the contents of the studied tablets differ significantly. Microcrystalline cellulose is one of the excipients that has been identified very frequently in both original and counterfeit samples of Viagra (see dark purple profiles in Figure 4a,e,f). Corn starch was observed much less frequently and only in the falsified samples—see gray profiles in Figure 4b,d. Other undeclared substances are also found in many samples of falsified Viagra tablets. From those found in our laboratory, calcium carbonate (calcite)—pink vertical lines in Figure 4c,f—is encountered very often, as well as calcium sulphate in differently hydrated forms, e.g., brown vertical lines in Figure 4e (here, we identified the anhydrous form—anhydrite—but very often gypsum and basanite can also be found).

3.2. Semiquantitative Analysis of Viagra 100 mg Tablets

3.2.1. Theory and General Concept

The examples in Figure 4 show that even dubious Viagra tablets from the illegal supply chain sometimes contain the proper API (examples in Figure 4b,d,e). They show, however, that the qualitative composition of the tablets differs significantly from the original product. As far as the differences are mainly in excipients, the question arises about the dose of API, which is a major issue when the health of a potential patient is concerned. In this case, both overdose as well as a lower dose is dangerous.

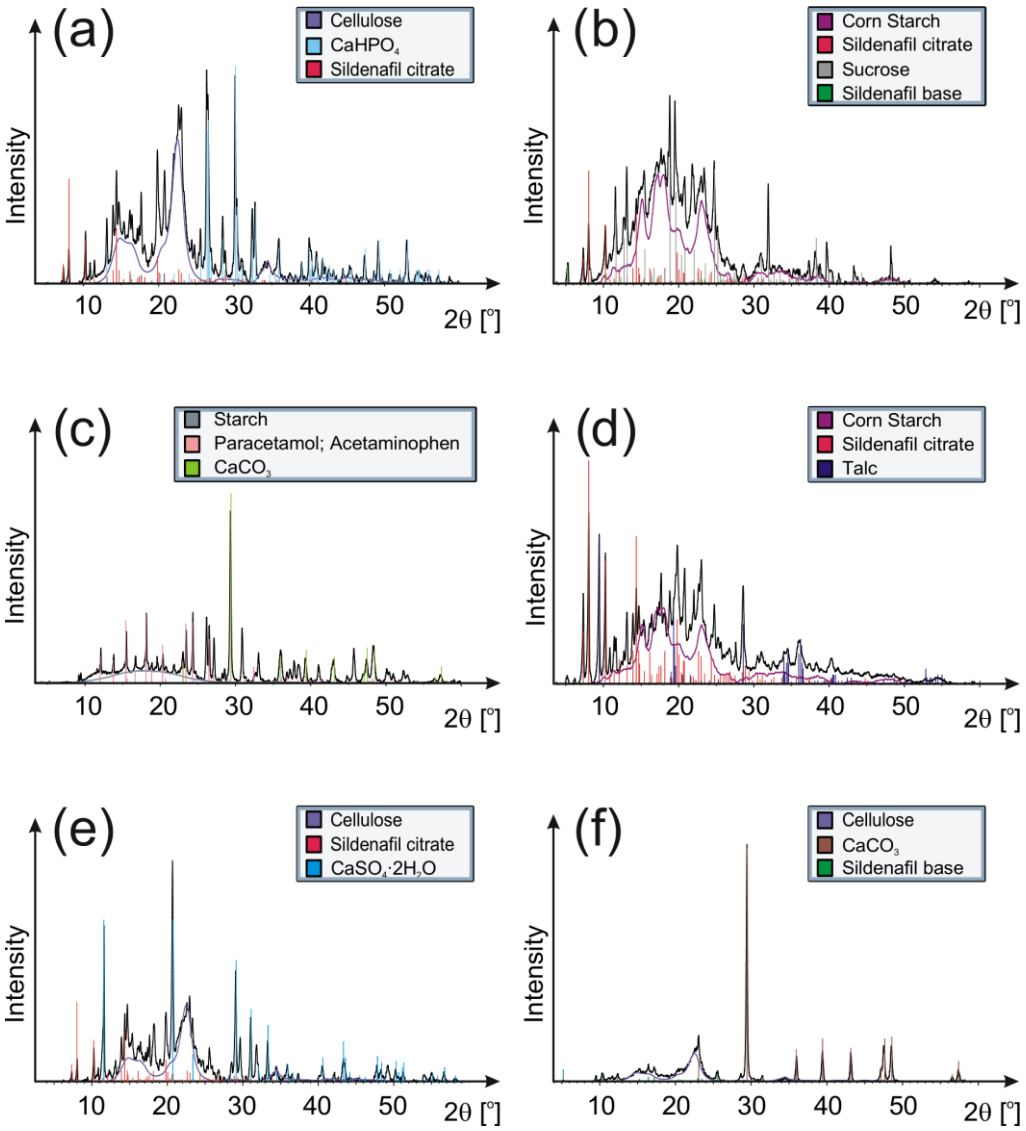

Figure 4. Examples of qualitative analyses of Viagra 100 mg tablets. (**a**) Original Viagra from Pfizer, (**b**–**f**) falsified products of different tablet compositions.

As was already mentioned before, the intensity of a reflection coming from an additive is proportional to its concentration in the sample. Because we usually use the same sample holders for the XRPD measurements, as well as the same protocol of analyses (at least we can perform analyses in such a way), the integral intensity of a reflection which is ascribed to a given crystalline phase gives us information about the concentration of this phase in the mixture. This is of course only true for regions where reflections from different phases do not overlap.

Generally, the integrated intensity of a diffracted peak (hkl) of a substance *i* measured with a diffractometer is: [35,36]

$$I_i = I_{pr} \cdot e^{-2Mi} \cdot p_i \cdot |F_i|^2 \cdot Lp \cdot \frac{Vi}{vi^2} \cdot T(\theta) \quad (1)$$

where:

I_{pr} = intensity of the primary beam;
e^{-2Mi} = Debye–Waller temperature factor;
p_i = multiplicity factor;
F_i = structure factor;
Lp = Lorentz–polarization factor;
V_i = volume of the compound *i* (pressed to the solid);
v_i = volume of the unit cell of a compound *I*;
$T(\theta)$ = transmitted fraction of the diffracted X-ray beam (dependent on θ, but not absorbed).

For the given conditions, some of the factors could be considered constant for a given (hkl) reflection and hence could be included in the K_i constant. Then, we obtain:

$$I_i = I_{pr} \cdot K_i \cdot V_i \cdot T(\theta) \quad (2)$$

or:

$$I_i = I_{pr} \cdot K_i \cdot \frac{M_i}{\rho_i} \cdot T(\theta) \quad (3)$$

because $M_i = \rho_i \cdot V_i$ where V_i is an effective volume. In practice, to obtain the value, a packing factor should be applied.

The transmitted fraction $T(\theta)$ is:

$$T(\theta) = e^{-\mu_m \rho l} \quad (4)$$

where μ_m = mass absorption coefficient, l = absorption path length and ρ = density of the sample.

The reasoning brings us finally to an equation:

$$C_i = I_i \cdot B_i \cdot \mu_m \quad (5)$$

which ties the concentration of the *i*-th phase with the intensity of the reflection. It assumes that for a given experimental conditions (diffractometer, divergence slits, sample area and thickness), some values for a reflection for the *i*-th phase (the subscripts A and B refer to the phases in a two-phase system) can be treated as being constant and written as B_i. The last equation shows also that the major problem in a very simple quantitative analysis of Viagra by an application of X-ray powder diffraction might be the differences in the mass absorption coefficients μ_m (see Tables A1 and A2) between unknown samples.

3.2.2. Quantitative X-ray Diffraction Methods

The general model and the straight line model are well-known quantitative methods based on Equation (5). Both methods can be used, when standard samples or calibration coefficients are available. Manuals for various X-ray instruments very often give two examples of quantitative analyses: the content of boehmite [AlO(OH)] in corundum (Al_2O_3), and of austenite in martensite (crystalline steel components containing iron and carbon). Both cases belong to the straight line model where μ_m is approximately the same for both components and hence μ_m is independent of sample compositions, which is unusually rare for our samples. This model is, however, suitable for evaluating different polymorph concentrations, which we have successfully applied several times in our lab.

We looked for a fast and simple-as-possible method of a quantitative X-ray analysis of sildenafil content in falsified erectile dysfunction medicinal products. We want to avoid

probe contamination by adding an internal standard in a quantitative approach. As we can see in exemplary diffractograms (Figures 3 and 4), products are mixtures of many phases including amorphous phases and ingredients characterized by overlapping peaks. Quantitative X-ray diffraction calculations based on crystallographic structures are difficult and sometimes impossible to apply. In contrast, methods based on the ratios of reflections' intensities (e.g., RIR) of different phases are not easily applicable due to the amorphous nature of some phases [28,36]. The straight line model has been selected as the starting point and "pure compounds" were used to prepare a series of two-phase samples for calibration curves. The samples used for calibration contained sildenafil citrate and a second phase. The second phase is one of the inactive substances that have been identified in previous qualitative analyses, such as calcium hydrogen phosphate ($CaHPO_4$), calcium carbonate ($CaCO_3$), calcium sulphate ($CaSO_4$), cellulose, starch, lactose, etc. In one case, as the second phase, a 1:1 mixture of calcium hydrogen phosphate and cellulose was applied which corresponds approximately to the composition of excipients in original Viagra products. Based on the intensities of reflections I_1 (for $2\theta \sim 7.3°$), I_2 ($2\theta \sim 8°$) and I_3 ($2\theta \sim 10.2°$) of sildenafil citrate, the respective calibration curves were prepared. The calibration curves for sildenafil citrate mixed with different excipients are shown in Figure 5.

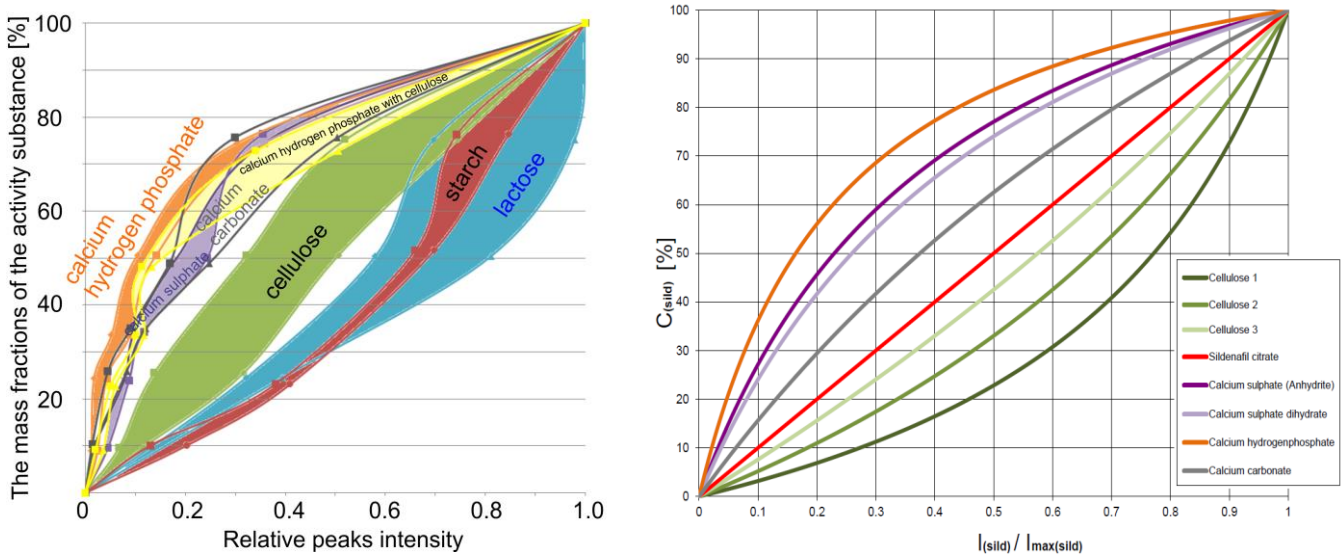

(**a**) (**b**)

Figure 5. Calibrations curves for two-phase samples containing sildenafil citrate: (**a**) on the basis of experimental measurements and (**b**) calculated calibrations curves (see Appendices D and E). Theoretical calibration curves have been calculated using data collected in Table A1 in Appendix B and the packing factor PF = 0.6 for both phases, except for $CaHPO_4$ where $PF_{Sildenafil\ citrate} = 0.4$, $PF_{CaHPO4} = 0.7$. Cellulose denoted 1: $PF_{Sildenafil\ citrate} = 1$, $PF_{Cellulose} = 0.4$; cellulose denoted 2: $PF_{Sildenafil\ citrate} = 0.6$, $PF_{Cellulose} = 0.4$; and cellulose denoted 3: $PF_{Sildenafil\ citrate} = 0.6$, $PF_{Cellulose} = 0.6$.

3.2.3. Generalization of the Linear Model

When the mass absorption coefficients of both phases (sildenafil citrate and second phase) in the sample are similar, then a straight line should be obtained as the calibration curve (Figure 5a). For organic substances such as lactose, starch or cellulose which have a lower μ_i than sildenafil citrate, the curves are below the straight line, whereas for inorganic substances such as calcium hydrogen phosphate, calcium hydrogen phosphate with

cellulose, calcium carbonate or calcium sulphate, the situation is reversed (see Table A1 in Appendix B). Therefore, instead of using linear regression, an equation is used:

$$C_A = \frac{100}{\frac{\mu_A \times PF_A}{\mu_B \times PF_B \times I_{rel}} - \frac{\mu_A \times PF_A}{\mu_B \times PF_B} + 1} \quad (6)$$

where $I_{rel} \neq 0$ and the packing factor $0 < PF < 1$ was derived and used to describe the calibration curves in Figure 5b (see Appendices D and E for transformations of equations and Figure A7).

3.3. A Semiquantitative Method Description

To determine the mass fraction of sildenafil citrate in the Viagra samples studied, the intensities of three reflections ascribed to sildenafil citrate were precisely measured (at a slower scanning speed and longer counting time—during the tests we wanted higher quality measurements than the standard qualitative analysis measurements in our laboratory) and the mass fraction was calculated applying the appropriate equation of the calibration curve. For lower sildenafil doses, the calibration curve can be approximated by a straight line which makes the approximation of the mass fraction even easier. The quantification is sometimes not very easy, because samples are composed of more than two phases. Therefore, to obtain more accurate result, an additional equation of calibration curve for a non-sildenafil citrate phase is necessary. Then, for both results, the final arithmetic mean can be calculated (see Appendix G for a standard deviation of the arithmetic mean). For a more accurate result, a new calibration curve for sildenafil citrate in the three-phase sample can be prepared. Nevertheless, the first step is always the qualitative analysis enabling the selection of a proper calibration curve. Then, selected reflections intensities have to be remeasured precisely and finally the mass fractions might be calculated.

The equation $C_A = f(I_A)$ was derived on the basis of theoretical considerations; however, in practice, interactions between phases are observed because of the physicochemical properties of the mixture. The properties can strongly depend on mass concentration. For example, a mixture that contains microcrystalline cellulose can swell. This behavior increases with the amount of microcrystalline cellulose in the sample (see Figures A2–A6 in Appendix C). However, the equation describes the calibration curve quite well in the range of the investigated concentrations of sildenafil. Calculations with this equation are easy with the use of the freeware GNUPLOT software, although a linear equation could also be used in a very narrow investigated range of concentrations (see Figure 2a,b and Appendix F). The intensities of selected reflection(s) for known phase concentrations are input as data variables to calculate the coefficients of the equation. Here, only the parameter A and the asymptotic standard error ΔA are determined. The standard error [%] gives an indication of the quality of the fit to experimental data. The A value can then be used for the inverse calculation to obtain estimated quantities of C_A based on the intensity of the reflection of the investigated powder sample.

The last step is to establish the dose of the active substance. To do so, we have to know the mass of the studied tablet.

3.3.1. Selected Calibration Curves and Input Data

We prepared calibration curves (i), (ii) and (iv) according to the below equation for the reflections mentioned previously. The calibration curves with the lower standard errors were selected for future mass estimation. We have reduced Equation (6) to Equation (7) in order to reduce the number of variables to a single parameter A that determines the behavior of the calibration curve, making it easier to calculate the fit. The parameter indicated by the italic capital letter A has its physical meaning as a ratio (see Equation (7) and Appendix E). The capital A is the parameter descriptor for the ratio of the mass absorption coefficients

and the packing factor of the two phases A and B (see Appendix E). More details including parameter A for the equation are collected in Table 1 and Appendix E.

$$C_A = \frac{100}{\frac{\mu_A \times PF_A}{\mu_B \times PF_B \times I_{rel}} - \frac{\mu_A \times PF_A}{\mu_B \times PF_B} + 1}, \text{ when } I_{rel} \neq 0. \quad (7)$$

An exemplary calibration curve is shown in Figure 2.

3.3.2. Results of Quantitative X-ray Estimation

Based on the relative intensities values presented in Table 1, we calculated the minimum (A_1) and maximum (A_2) values of the parameter A by applying an asymptotic standard error. We used the following equations $A_1 = A - \Delta A$ and $A_2 = A + \Delta A$.

C_{A1} and C_{A2} were calculated for Equation (7) using A_1 and A_2, respectively, for each intensity. The lowest and the highest C_{A1} and C_{A2} for the same sample were selected for future calculations and the final $C_A \pm \Delta C_A$ values were calculated, where $C_A = (C_{A1} + C_{A2})/2$ and $\Delta C_A = |C_A - C_{A1}|$.

Table 1. The A parameter and standard errors obtained for selected calibration curves: (i) sildenafil citrate in calcium sulphate dihydrate, (ii) sildenafil citrate in microcrystalline cellulose and (iv) calcium sulphate dihydrate in microcrystalline cellulose.

Mixture	2θ Angle	A	Asymptotic Standard Error ΔA	Standard Error [%]
(i)	~8.2°	0.397885	0.007359	1.85
(ii)	~8.2°	0.535955	0.01679	3.13
(iv)	~11.6°	0.595521	0.01895	3.18

The relative intensities calculated and used for further calculations are in Appendix K in Tables A5 and A6. The estimated concentrations and masses of calcium sulphate and sildenafil citrate on the basis of calibrations curves (i), (ii) and (iv) are collected in Tables 2–4.

Table 2. Estimated concentrations and masses of calcium sulphate (the calibration curve (iv) for the mixture of calcium sulphate dihydrate in microcrystalline cellulose).

	Concentration [%]		Mass [mg]	
Sample	**Nominal**	**Found $C_A \pm \Delta C_A$**	**Nominal**	**Found**
C01	4.91	9.7 ± 0.4	22.7	44.7
C02	26.13	28.8 ± 0.7	141.3	155.9
C03	26.69	31.4 ± 3.2	114.6	134.6
Calcium sulphate dihydrate	100.00	99.6 ± 0.0		

Table 3. Estimated masses of sildenafil citrate calculated with calibration curves for (i) sildenafil citrate in calcium sulphate dihydrate, (ii) sildenafil citrate in microcrystalline cellulose and (v) A_{mean} after the improvement in quantitative X-ray estimation.

Sample	Nominal Mass [mg]	Found Mass [mg]		
		(i)	**(ii)**	**(v)**
C01	74.556	89.2	69.5	78.3
C02	44.992	60.0	45.9	52.1
C03	87.248	84.2	65.9	73.9

Table 4. Estimated concentrations of sildenafil citrate calculated using the XRPD method (calibration curves for (i) sildenafil citrate in calcium sulphate dihydrate, (ii) sildenafil citrate in microcrystalline cellulose and (v) A_{mean} after corrections of quantitative XRPD estimation), DAD and MS methods.

Sample	Nominal Concentration [%]	Found Concentration $C_A \pm \Delta C_A$ [%]				
		XRPD (i)	XRPD (ii)	XRPD (v)	DAD	MS
Sildenafil	100.00	100.0 ± 0.6	99.9 ± 0.7	100 ± 0.7	n.m.	n.m.
F01	unknown	16.6 ± 0.3	12.9 ± 0.4	14.5 ± 0.3	19.07 ± 0.22	18.77 ± 0.22
F02	unknown	7.3 ± 0.4	5.6 ± 0.4	6.3 ± 0.4	15.83 ± 1.43	16.68 ± 1.90
C01	16.13	19.3 ± 0.5	15.0 ± 0.6	16.9 ± 0.6	15.20 ± 0.04	15.53 ± 0.06
C02	8.32	11.1 ± 0.7	8.5 ± 0.6	6.9 ± 0.7	8.13 ± 0.01	8.37 ± 0.01
C03	20.32	19.6 ± 0.3	15.3 ± 0.4	17.2 ± 0.4	19.19 ± 0.33	19.64 ± 0.07

n.m.—not measured.

3.3.3. Correction of Quantitative X-ray Estimation by Determination of A_{mean}

The aforementioned analysis was based on two phases' curves, whereas in real samples there is a mixture of three or more phases. One can presume that quantitative calibration curve for sildenafil should have a shape somewhere between these two described calibrations curves; in this case, for sildenafil citrate with calcium sulphate and the calibration curve with microcrystalline cellulose (Figure 5). Then, instead of A we obtain an A_{mean}, according to the equation:

$$A_{mean} = \frac{A_{\text{sildenafil citrate from calcium sulphate}} + A_{\text{sildenafil citrate from microcrystalline cellulose}}}{2}$$

$$\Delta A_{mean} = \left|\frac{\partial y}{\partial x}\right||\Delta A_1| + \left|\frac{\partial y}{\partial x}\right||\Delta A_2| = \frac{1}{2}|\Delta A_1| + \frac{1}{2}|\Delta A_2|$$

In our example, A_{mean} is equal to (0.397885 + 0.535955)/2 = 0.46692 with ΔA_{mean} = (0.007359 + 0.01679)/2 = 0.0120745; therefore, there are two border values A_{1mean} = 0.4548455 and A_{2mean} = 0.4789945. A_{mean} is a value for a "virtual calibration curve" for a mixture of three phases calculated from A values for curves (i) and (ii). The final mass and concentration values are summarized in Tables 3 and 4.

We performed many different XRPD quantitative estimations of samples containing different excipients. Here, we have presented only results for a very common mixture of sildenafil citrate with gypsum and cellulose. Our estimated values of sildenafil citrate in Table 4 are quite close to the nominal masses or nominal concentrations.

3.4. LC-DAD and LC-QTOF-MS Methods Validation

The RSDs of the retention time were 0.09% with DAD and 0.11% with MS detection and the mean mass error was −3.6 ppm. There were not any interferences observed on DAD and MS chromatograms. Parallel detection using two techniques allows us to verify the purity of peaks present on UV chromatograms. The signals of DAD and MS detection were linear in the range from 0.4 to 14 μg·mL^{-1} (r^2 = 0.9989) and from 0.08 to 20 μg·mL^{-1} (r^2 = 0.9961), respectively. Intra- and inter-day precision and accuracy data are presented in Table A4 in Appendix I. Both methods were precise, accurate and linear in a range from 5 to 13 μg·mL^{-1}. Established methods were applied as reference methods to quantify the content of sildenafil in selected samples. The results of the XRPD estimations are also similar to the results obtained with the DAD and MS methods (Table 4).

3.5. LOQ and LOD of XRD

The limit of quantitation (LOQ) and limit of detection (LOD) depend on the composition of the sample, how the sample is prepared for measurement and how accurate the measurement is—the measurement time changes the difference between the desired signal and the background. It also depends on what reflection observations have been made. For the LOD, we took peak intensities (calculated as the difference between the maximum of the peak and the background) greater than three standard deviations, determined as

the noise of the background around the peak. For the LOQ, the intensity of the peak was six times greater than the background noise. Eventually, we decided that the noise in the background would be calculated twice for a maximum of the intensity of peak, on the left and the right side of each peak, for the same measurement, instead of noise for the "blank sample" in the place where the reflection should be present. Moreover, it is worth noting that for LOD and LOQ, the maximum intensities of the peak were taken; however, semi-quantities analyze the field under the peak. This is important information because from time to time, a different shape of peaks was observed for the same sample, where maximum intensities were significantly different; nevertheless, the area of the peak was often quite similar.

Measurements were repeated several times for the same sample with a well-defined amount of sildenafil citrate in mixtures. There are variations in the intensities of background and reflections for sildenafil citrate in calcium sulphate and mixtures with microcrystalline cellulose. A visualization of data and summary are in Figures A10–A14 and Table A3 in Appendix H. There are variations in the intensities of background and reflections for sildenafil citrate in calcium sulphate and mixtures with microcrystalline cellulose.

The LOD was about 3–6% for sildenafil citrate in calcium sulphate and about 1–3% for sildenafil citrate in microcrystalline cellulose when using conventional phase identification measurements. For the XRD measurements used in our semi-quantitative study, the LOQ was determined. We analyzed the intensities of three peaks located at ~7.2°, ~8° and ~10.6°. The LOQ was determined to be ~3%, 1–6% and ~3–6%, respectively, for selected peaks of sildenafil citrate in calcium sulphate. For sildenafil citrate in cellulose, the LOQ was determined to be ~1%, ~1–3% and ~1%, respectively. Although the LOQ for different peaks varies, the LOQ for measurements with the settings used for our semi-quantitative analysis is lower than the LOD for qualitative analysis.

3.6. Summary

Data obtained from X-ray experiments were correlated with results from validated liquid chromatography coupled to a diode array detector and mass spectrometry techniques. The intra- and inter-day variance of the semiquantitative X-ray powder diffraction analysis method was determined by constructing a new set of two calibration curves. One curve is for sildenafil citrates in microcrystalline cellulose and another for sildenafil citrate in gypsum (Appendix H). The shape of the calibration curve for sildenafil citrate in microcrystalline cellulose is different from the shape of the calibration curve for sildenafil citrate in gypsum.

The difference in shape between the two types of mixtures is expected based on the equation for C_A and based on expectations from experiments (see Figure 5 and Appendices C and D). There are two mixtures, both of which have different compositions, including density (as a consequence, the mass absorption coefficients for each compound are different in this case) and the packing factor of the crystals, and there may also be a preferred orientation of the crystals in the powder sample. All these elements (according to the equation for C_A) affect the shape of the calibration curve. On certain curves, particular points have sometimes been omitted because of the economic aspect of sildenafil citrate, e.g., points 0.4 or 0.8 contain about 40–80% of sildenafil citrate. On the other hand, we do not expect such a high concentration of sildenafil in medicines or fake medicines.

4. Discussion

A semi-quantitative method of sildenafil content determination using simple X-ray diffraction analysis has been presented. An example of a product containing microcrystalline cellulose and gypsum (calcium sulphate dihydrate) in addition to the API was presented. The use of gypsum was taken into account because of the very frequent occurrences of this compound in falsified Viagra products. The obtained results were additionally compared to results obtained by two validated methods of quantitative sildenafil analyses. Hence, during a phase identification process, we can also determine more or less

the accurate amounts of sildenafil in a drug or counterfeit medicine. The obtained results seem to be satisfactory for a preliminary quantification of the API dose, which is very important for establishing health risks for the prospective patient. In the course of studies, we established the importance of radiation absorption in a sample. The proposed method is time- and apparatus-independent and the obtained calibration curves can be used for all samples of similar qualitative composition. Moreover, in our opinion, it can be also used for sildenafil content estimations in the case of samples composed of excipients having similar and not-identical mass absorption coefficients as gypsum.

The method has its deficiencies, the errors of concentration estimations are pretty high and the results can be used only as an indication of falsification and plausible health-threat of the product, especially with a lack of the original sample. In the latter case, the comparison of diffraction patterns of dubious and original products gives an easy and fast answer. There are some difficulties with this method that affect the final result. The main problem is the intensity for 100% of the API against which the other relative intensities are calculated. Sometimes it is not easy to obtain the intensity of the reflection from the diffractogram. This is due to overlapping reflections: different layers of the same phase have similar d values or reflections from different phases have similar d values. Some products, especially in certain concentration ranges of multiphase systems, may have a sample texture. This will affect the intensity of the reflection.

We demonstrated that in powder diffraction, absorption is not the only parameter which affects the reflection intensity-concentration proportionality. The degree of powder packing and compression (PF) is an important factor. However, our proposed parameter A includes both the packing factor and the mass absorption coefficient. The PF factor can correct for errors in the determination of the absorption coefficient. Thus, the first question was: does sildenafil citrate contain water molecules in the crystal structure and is it sildenafil citrate monohydrate? A comparison of the diffraction patterns for crystal structures (sildenafil citrate monohydrate, sildenafil citrate hemihydrate [37,38]) and the diffraction pattern from the ICDD database (PDF 00-052-2420 later published in [39]) shows that they are somewhat similar. The diffraction patterns of both these and other close compositions are similar for many strong reflections, so there is no point in time-consuming examinations (see Figures A17 and A18 in Appendix L). In addition, the study of heating sildenafil citrate monohydrate up to 200 °C was conducted earlier and it can be seen that the intensity of reflections changes significantly around 2θ ~ 7° and ~12° 13.5° for Cu$K\alpha$ radiation [40] (please compare with our investigations in Figure A18). All calculations were performed for sildenafil citrate powder without water content, which cannot be excluded due to the absorption of water from the air, under the assumption that we are using an API standard of sildenafil citrate (Appendices A and B).

We postulate that Figure 5a additionally shows that the substances can be exchanged for another, e.g., in the multiphase system the composition can be exchanged like calcium hydrogen phosphate for calcium sulphate or calcium carbonate or into two mixtures of compounds of calcium hydrogen phosphate with cellulose. Then, as long as the reflections from the different phases do not overlap significantly, using parameter A in a given concentration range should still allow the concentration to be estimated fairly well from the intensity of the reflection without the need for a new calibration curve.

The step size and the time per step affect the intensity value. These parameters should be set individually for the experimental configuration to obtain the best ratio between LOD or LOQ and total data collection time (Figures A15 and A16 in Appendix J). The step size depends on the full width at half maximum (FWHM) of the reflection. The well-known rule of at least eight points above the FWHM of the reflection seems to be appropriate. It is best to measure the background to the left and right of the reflection for at least six FWHMs (three reflections) when measuring or selecting an individual reflection.

The intensity of the reflectance for pure API should be measured and corrected from time to time due to, among other things, the wear of the X-ray tube.

It takes time to construct the calibration curve, determine the parameter A for the equations $C_A = f(I_A)$ and verify the results.

The method can also be worked out for completely different pharmaceutical products, although it must be stated that it is restricted only to those products of relatively high API concentrations/doses of good crystalline character and hence giving strong X-ray diffraction. Advantageously, the calibration curves (Figures A7, A9 and 5a,b) can be easily corrected by changing parameter A; for example, by calculating the average value of parameter A (see Tables 1 and 4).

5. Conclusions

The linear regression equation has been derived and generalized to the non-linear regression equation where the coefficients have crystallographic significance. It should be emphasized that this method is not intended to compete with LC-DAD or LC-QTOF-MS. The semi-quantitative method can only be used as a first estimation, after which, if necessary, a well-established and accurate quantification by LC-DAD and LC-QTOF-MS can be performed. On the other hand, this work aims to provide the scientific community with a general formula that allows the use of a calibration curve for a two-component system using non-linear regression. Researchers are encouraged to develop their own semi-quantitative curves for various powder products. The authors believe that despite these rough estimates, the simple and rapid feedback of quantitative information may be useful in detecting counterfeits that pose a high health risk to patients/consumers.

The A parameter must be determined for the appropriate phase system and measurement conditions. This takes time and requires reagents to obtain calibration curve(s) but, once done, the A parameter can be used permanently for semi-quantitative estimation as long as the measurement conditions are not changed. This prevents contamination of an evidential sample with external standards. This is critical for evidence material, so that it can be used in the future for repeat measurements or other analyses. A summary of the semi-quantitative X-ray powder diffraction analysis described here is shown in Figure 1 as a graphical representation of the algorithm.

Author Contributions: Conceptualization, J.K.M. and K.P.-S.; Data curation, A.B. (Armand Budzianowski), K.P.-S.; Formal analysis, A.B. (Armand Budzianowski), K.P.-S., A.B. (Agata Błażewicz) and M.P.; Funding acquisition J.K.M. and A.B. (Armand Budzianowski); Investigation, A.B. (Armand Budzianowski), K.P.-S., A.B. (Agata Błażewicz) and M.P.; Methodology: A.B. (Armand Budzianowski), J.K.M. and K.P.-S.; Project administration, J.K.M.; Resources, J.K.M. and A.B. (Agata Błażewicz); Software, A.B. (Armand Budzianowski); Supervision, J.K.M.; Validation, K.P.-S., J.K.M., M.P., A.B. (Agata Błażewicz) and A.B. (Armand Budzianowski); Visualization, A.B. (Armand Budzianowski), writing—original draft preparation, A.B. (Armand Budzianowski), A.B. (Agata Błażewicz), M.P., J.K.M. and K.P.-S.; Writing—review and editing, A.B. (Armand Budzianowski) and J.K.M. The XRD technique was used by: A.B. (Armand Budzianowski), J.K.M. and K.P.-S., while the LC-DAD and the LC-QTOF-MS techniques were used by A.B. (Agata Błażewicz) and M.P. All authors have read and agreed to the published version of the manuscript.

Funding: This study is a fragment of the project of the National Medicines Institute supported with statutory subsidies by the Ministry of Science and Higher Education of the Republic of Poland.

Data Availability Statement: The data presented in this study are available in the article or appendices.

Conflicts of Interest: The authors declare no conflict of interest.

Appendix A

Data used in the article.

- 100 mg of sildenafil is equal to ~140.5 mg of sildenafil citrate;
- 100 mg of sildenafil citrate is equal to ~71.2 mg of sildenafil;
- The molar mass of sildenafil citrate ($C_{28}H_{38}N_6O_{11}S$) is 666.70 g/mol;
- The molar mass of sildenafil ($C_{22}H_{30}N_6O_4S$) is 474.58 g/mol.

Appendix B

Data used in the article are in Table A1. The mass absorption calculation example is in Table A2.

Table A1. Mass absorption coefficients (cm^2/g) for selected substances. Based on Table 4.2.4.3 "Mass attenuation coefficients" on page 200 in [41], the following values (for CuKα radiation) were used for calculations: for H, 0.39 cm^2/g; for C, 4.51 cm^2/g; for N, 7.44 cm^2/g; for O, 11.50 cm^2/g; for Ca, 29.70 cm^2/g; for P, 75.50 cm^2/g; for S, 93.30 cm^2/g; for Si, 63.70 cm^2/g. Exemplary calculations are in Table A2.

Compound Name	Sum Chemical Formula	Molar Mass	Mass Absorption Coefficient (cm^2/g)
a-Lactose monohydrate	$C_{12}H_{24}O_{12}$	360.312	7.95803
Cellulose (D-Glucose)	$(C_6H_{12}O_6)_n$	n · 180.156	7.95803
Starch (D-Glucose)	$(C_6H_{12}O_6)_n$	n · 180.156	7.95803

Table A1. *Cont.*

Compound Name	Sum Chemical Formula	Molar Mass	Mass Absorption Coefficient (cm^2/g)
Sildenafil [42] *	$C_{22}H_{30}N_6O_4S$	474.576	11.70811
Sildenafil citrate	$C_{28}H_{38}N_6O_{11}S$	666.700	10.75821
Sildenafil citrate monohydrate [37] **	$C_{28}H_{38}N_6O_{11}S \cdot 1H_2O$	684.715	10.74502
Sildenafil citrate hemihydrate [38] ***	$C_{28}H_{38}N_6O_{11}S \cdot 1/2H_2O$	675.707	10.75153
Calcium carbonate	$CaCO_3$	100.087	17.94904
Calcium hydrogen phosphate	$CaHPO_4$	136.057	31.34856
Calcium sulphate dihydrate (*Gypsum*)	$CaSO_4 \cdot 2H_2O$	172.171	30.71089
Calcium sulphate hemihydrate (*Bassanite*)	$CaSO_4 \cdot 1/2H_2O$	290.297	34.51880
Anhydrous calcium sulphate (*Anhydrite*)	$CaSO_4$	136.141	36.12408
Silicon dioxide	SiO_2	60.084	35.90010

* The reference is to the crystal structure of 5-(2-Ethoxy-5-(4-methylpiperazin-1-yl-sulfonyl)phenyl)-2-methyl-3-propyl-6,7-dihydro-2H-pyrazolo[4,3-d]pyrimidin-7-one. ** The reference is to the crystal structure of 1-((3-(6,7-Dihydro-1-methyl-7-oxo-3-propyl-1H-pyrazolo(4,3-d)pyrimidin-5-yl)-4-ethoxy phenyl)sulfonyl)-4-methylpiperazinium citrate monohydrate at 120 K. *** The reference is to the crystal structure of 1-([3-(6,7-Dihydro-1-methyl-7-oxo-3-propyl-1H-pyrazolo[4,3-d]pyrimidin-5-yl)-4-ethoxyphenyl]sulfonyl)-4-methylpiperazinium citrate hemihydrate at 173 K.

Table A2. An exemplary calculation of mass absorption coefficients for sildenafil citrate $C_{28}H_{38}N_6O_{11}S$.

Element	Atomic Mass [u] or [g/mol]	Number of Atoms in Molecule	Sum of Atomic Masses [g/mol]	Ratio to Total Mass	Mass Attenuation Coefficient for CuKα [cm^2/g]	Mass Absorption Coefficient for CuKα Radiation [cm^2/g]
C	12.0107	28	336.30	0.018015	4.51	$28 \cdot 0.018015 \cdot 4.51 = 2.274953319$
H	1.00794	38	38.30	0.001512	0.39	$38 \cdot 0.001512 \cdot 0.39 = 0.022405389$
N	14.0067	6	84.04	0.021009	0.021009	$6 \cdot 0.021009 \cdot 0.021009 = 0.937841852$
S	32.065	1	32.07	0.048095	93.3	$1 \cdot 0.048095 \cdot 93.3 = 4.487272925$
O	15.9994	11	175.99	0.023998	11.5	$11 \cdot 0.023998 \cdot 11.5$ 3.035734728
Total (sum)	-	-	666.6999	-	-	10.7582

Appendix C

XRPD patterns of exemplary compounds were superimposed to select reflections for the calibration curve and semi-quantity estimation. For diffractograms and exemplary calculation curves for data that were used as an example in the text, see Figures A1–A6.

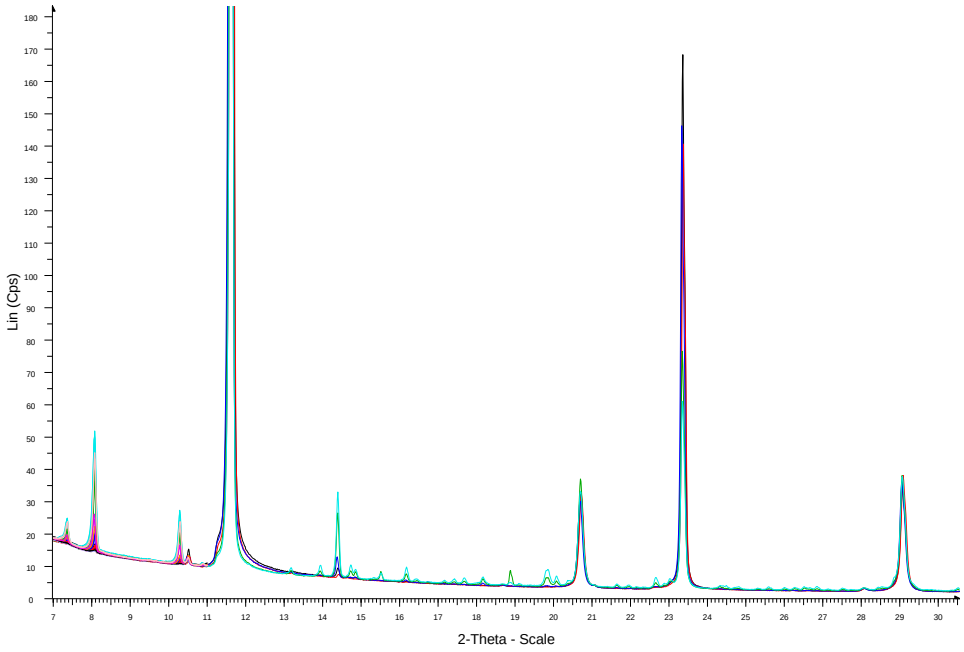

Figure A1. Diffractograms of sildenafil citrate/gypsum mixtures with different ratios.

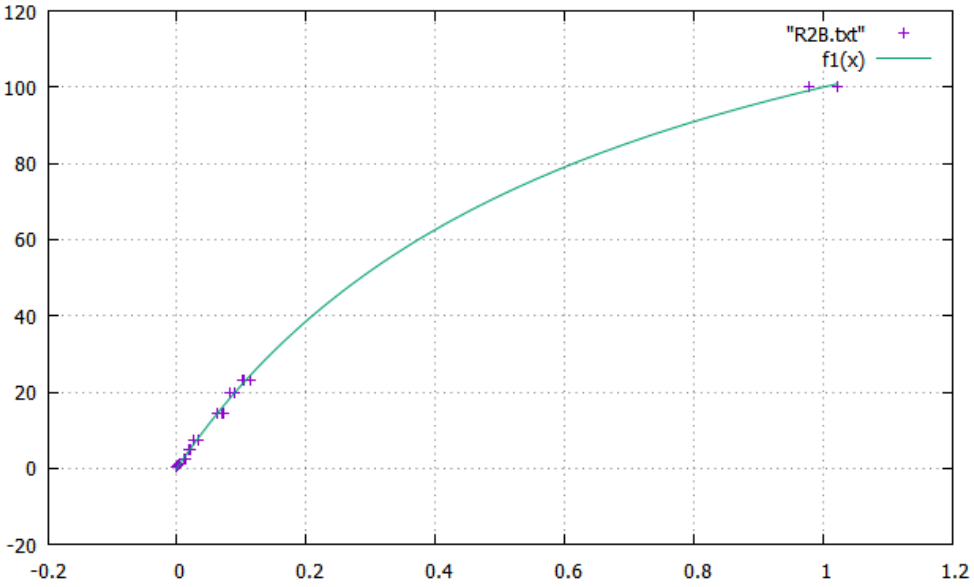

Figure A2. The calibration curve (i) of sildenafil citrate in gypsum.

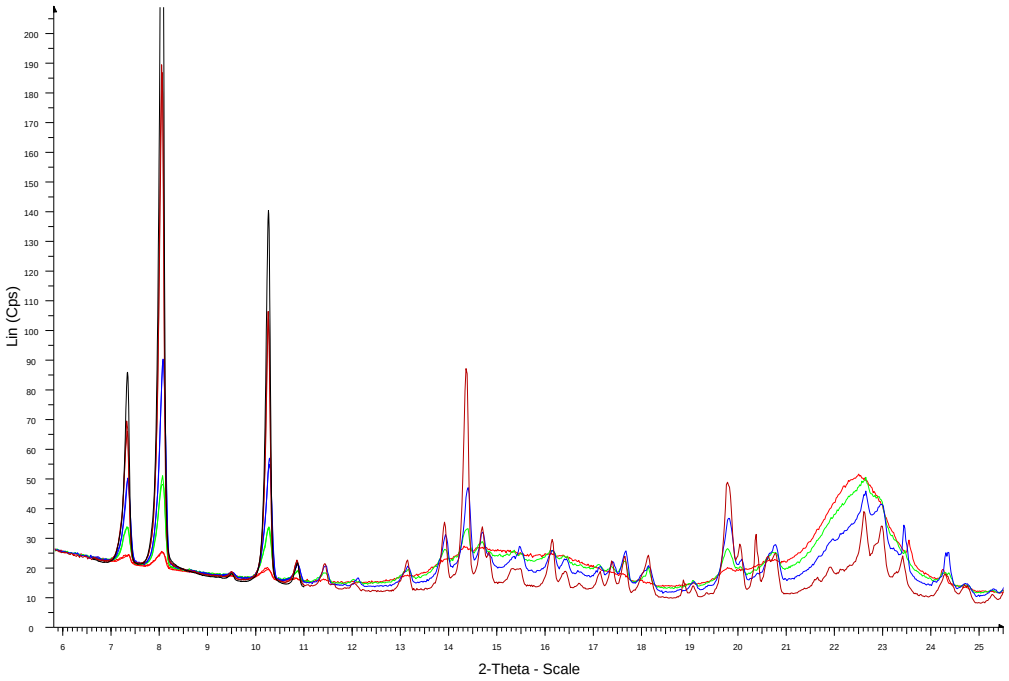

Figure A3. Diffractograms of sildenafil citrate/microcrystalline cellulose mixtures with different ratios.

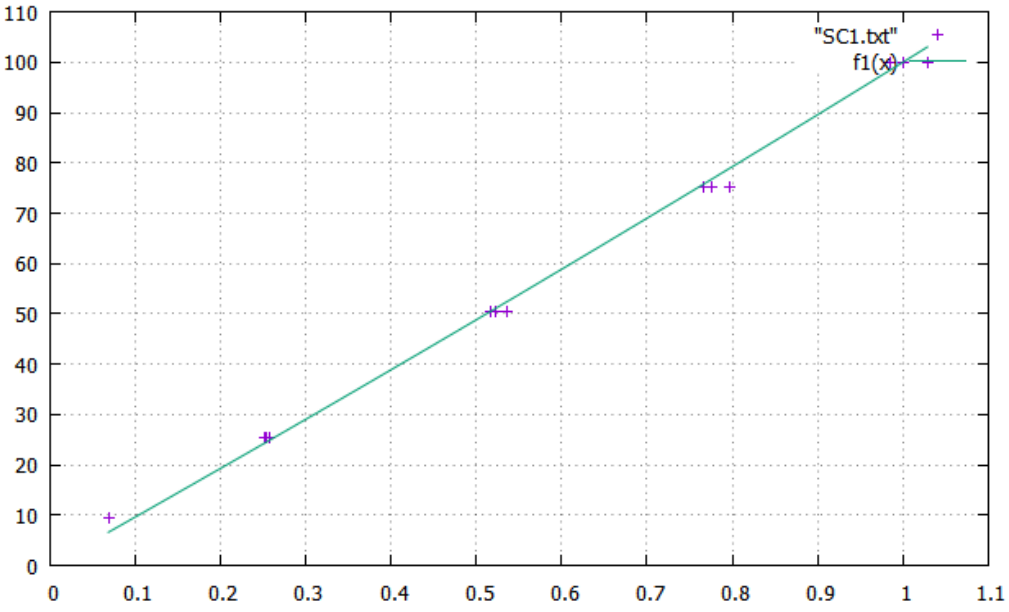

Figure A4. The calibration curve (ii) of sildenafil citrate in microcrystalline cellulose.

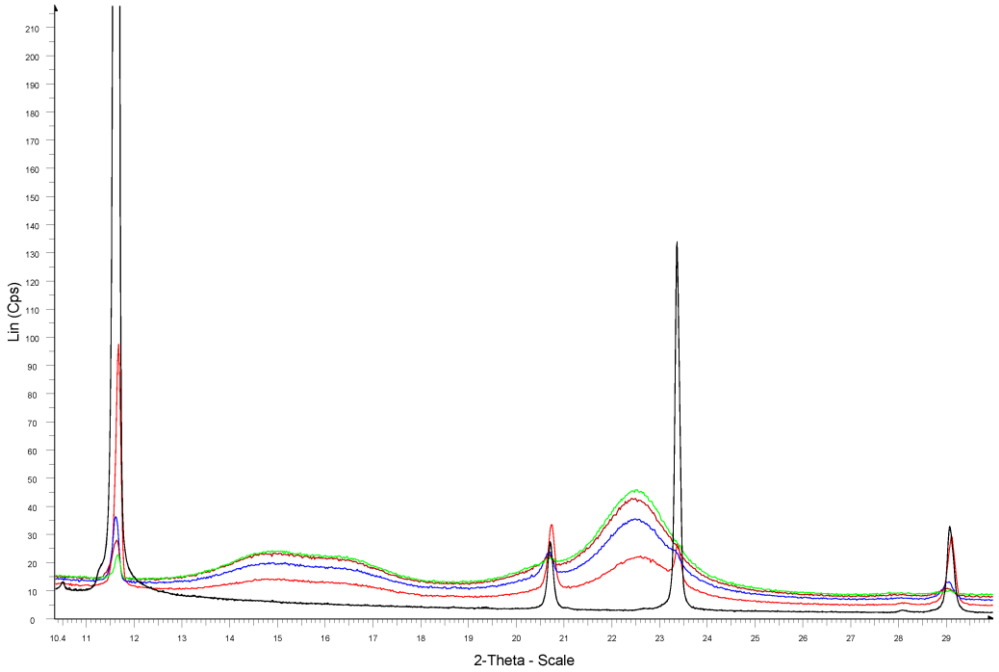

Figure A5. Diffractograms of sildenafil gypsum/microcrystalline cellulose mixtures with different ratios.

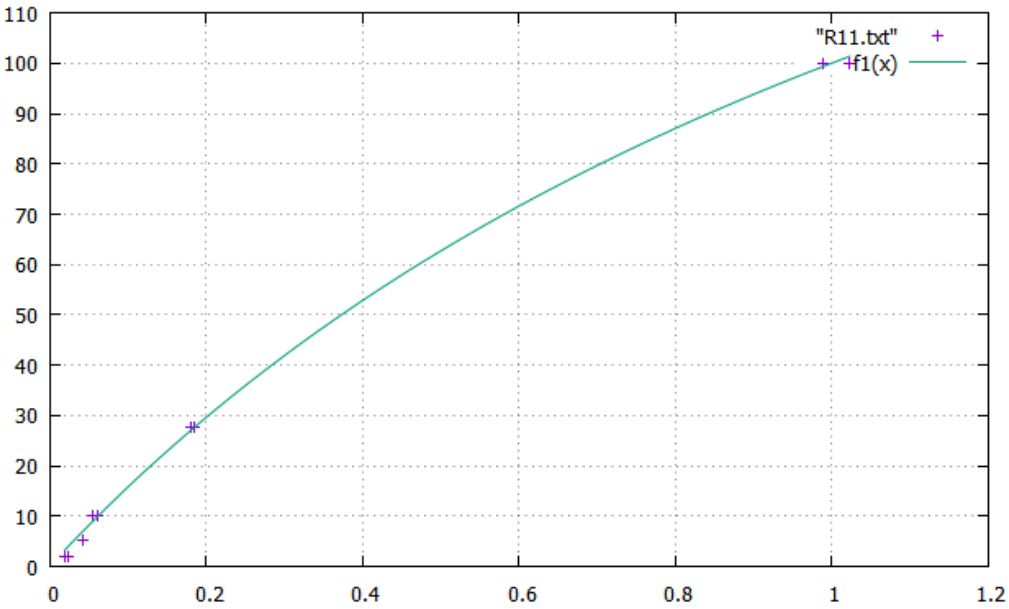

Figure A6. The calibration curve (iv) of gypsum in microcrystalline cellulose.

Appendix D

On the basis of equation $C_A = I_A \times B \times \mu_m$, where B is determined by calibration, mass absorption coefficients μ_m for all samples must be taken into consideration. The letters A and B in the subscript indicate phase A or B in a two-phase system. Therefore $I_A = \frac{C_A}{B \times \mu_m}$, where $\mu_m = \frac{C_A}{100} \times \mu_A \times PF_A + \frac{100-C_A}{100} \times \mu_B \times PF_B$. And eventually $I_A = \frac{C_A}{B \times \left(\frac{C_A}{100} \times \mu_A \times PF_A + \frac{100-C_A}{100} \times \mu_B \times PF_B\right)}$.μ stands for mass absorption coefficient (cm^2/g), see Table A1 in Appendix B.

PF stands for the packing factor between 0 and 1 and should be determined; however, the real value for the powder should be around 0.4 to 0.8 and depends on the powder properties that can determine the packing of the powder.

In the case of a pure active substance, C_A is equal to 100%. Thus, $I_{A100\%} = \frac{100}{B\times\left(\frac{100}{100}\times\mu_A\times PF_A+\frac{100-100}{100}\times\mu_B\times PF_B\right)}$, and therefore the formula shortens to $I_{A100\%} = \frac{100}{B\times(\mu_A\times PF_A)}$.

The calibration curve is $f(x) = I_{relA}(C_A)$. However, to determine C_A on the basis of I_{relA} from a diffractogram, the following transformations of the equation have been applied: $I_{relA} = \frac{I_A}{I_{A100\%}}$

$$I_{relA} = \frac{\frac{C_A}{B\times\left(\frac{C_A}{100}\times\mu_A\times PF_A+\frac{100-C_A}{100}\times\mu_B\times PF_B\right)}}{\frac{100}{B\times\mu_A\times PF_A}}$$

$$I_{relA} = \frac{C_A}{B\times\left(\frac{C_A}{100}\times\mu_A\times PF_A+\frac{100-C_A}{100}\times\mu_B\times PF_B\right)}\times\frac{B\times\mu_A\times PF_A}{100}$$

$$I_{relA} = \frac{C_A\times\mu_A\times PF_A}{100\times\left(\frac{C_A}{100}\times\mu_A\times PF_A+\frac{100-C_A}{100}\times\mu_B\times PF_B\right)}$$

$$I_{relA} = \frac{C_A\times\mu_A\times PF_A}{C_A\times\mu_A\times PF_A+(100-C_A)\times\mu_B\times PF_B}$$

$$C_A\times\mu_A\times PF_A = I_{relA}\times[C_A\times\mu_A\times PF_A+(100-C_A)\times\mu_B\times PF_B]$$

$$C_A\times\mu_A\times PF_A = I_{relA}\times C_A\times\mu_A\times PF_A+(100-C_A)\times I_{relA}\times\mu_B\times PF_B$$

$$\frac{C_A\times\mu_A\times PF_A}{I_{relA}\times\mu_B\times PF_B} = \frac{C_A\times\mu_A\times PF_A}{\mu_B\times PF_B}+(100-C_A)$$

$$(100-C_A) = \frac{C_A\times\mu_A\times PF_A}{I_{relA}\times\mu_B\times PF_B}-\frac{C_A\times\mu_A\times PF_A}{\mu_B\times PF_B}$$

$$100 = \frac{C_A\times\mu_A\times PF_A}{I_{relA}\times\mu_B\times PF_B}-\frac{C_A\times\mu_A\times PF_A}{\mu_B\times PF_B}+C_A$$

$$100 = C_A\left[\frac{\mu_A\times PF_A}{I_{relA}\times\mu_B\times PF_B}-\frac{\mu_A\times PF_A}{\mu_B\times PF_B}+1\right]$$

$$C_A = \frac{100}{\frac{\mu_A\times PF_A}{\mu_B\times PF_B\times I_{relA}}-\frac{\mu_A\times PF_A}{\mu_B\times PF_B}+1}$$

$$C_A = \frac{100}{\frac{A}{I_{relA}}-A+1},\ \text{for}\ A = \frac{\mu_A\times PF_A}{\mu_B\times PF_B},\ \text{when}\ I_{relA}\neq 0.$$

Appendix E

The calibration curve $f(x) = I_{relA}(C_A)$ is:

$$C_A = \frac{100}{\frac{A}{I_{rel}}-A+1},\ A = \frac{\mu_A\times PF_A}{\mu_B\times PF_B}\ \text{and}\ PF_A+PF_B\leq 1(\text{usually between 0.4 to 0.7})$$

$$C_A = \frac{100}{\frac{\mu_A\times PF_A}{\mu_B\times PF_B\times I_{rel}}-\frac{\mu_A\times PF_A}{\mu_B\times PF_B}+1},\ \text{when}\ I_{rel}\neq 0.$$

μ stands for the mass absorption coefficient (cm^2/g) (see Table A1 in Appendix B), which is significantly different from the linear absorption coefficient (mm^{-1}). μ is easy to calculate for monocrystals and the total packing factor (PF) is between 0 and 1 and

should be determined. However, the real value for the powder should be around 0.4 to 0.8 depending on the powder properties that can determine the packing of the powder.

$$A = \frac{\mu_A \times PF_A}{\mu_B \times PF_B} \tag{A1}$$

$$\frac{PF_A}{PF_B} = A\frac{\mu_B}{\mu_A} \text{ and } PF_A + PF_B \leq 1 (\text{usually between 0.4 to 0.7})$$

Let us assume that $PF_B = PF_{total} - PF_A = 0.7 - PF_A$.

$$\frac{PF_A}{0.7 - PF_A} = A\frac{\mu_B}{\mu_A}$$

$$PF_A = (0.7 - PF_A) \times A\frac{\mu_B}{\mu_A}$$

$$PF_A = 0.7 \times A\frac{\mu_B}{\mu_A} - A\frac{\mu_B}{\mu_A}PF_A$$

$$PF_A + A\frac{\mu_B}{\mu_A}PF_A = 0.7 \times A\frac{\mu_B}{\mu_A}$$

$$PF_A\left(1 + A\frac{\mu_B}{\mu_A}\right) = 0.7 \times A\frac{\mu_B}{\mu_A}$$

$$PF_A = \frac{0.7 \times A\frac{\mu_B}{\mu_A}}{\left(1 + A\frac{\mu_B}{\mu_A}\right)}$$

Eventually $PF_A = \frac{FP_{total} \times A\frac{\mu_B}{\mu_A}}{\left(1+A\frac{\mu_B}{\mu_A}\right)}$, where FP_{total} could be between 0 and 1; however, usually it is between 0.4 and 0.7.

Function graphs for different values of A parameters are compiled in Figure A7 below.

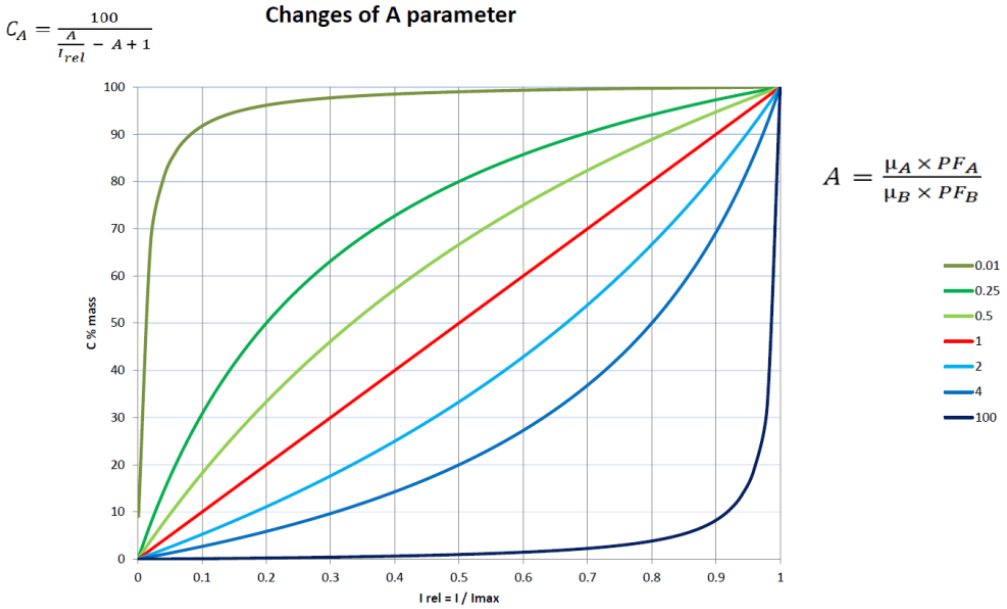

Figure A7. Function graphs for different values of the A parameter.

Appendix F

Following the commands of GNUPLOT allows us to fit the curve to the data in a file "data.txt". The data.txt file contains two columns of data, separated by a tabulator. The first column is for intensity, whereas the second stands for the mass concentration (%). The first command is a definition of the equation. In the second line, the initial value for a variable is assigned. The start of the calculation is in row three. In the last line is a command to show a plot on the basis of the previous calculations and data in the data.txt file. These four commands can be saved in the file with the "plt" extension (e.g., name_of_file.plt) for a future simpler approach, using the command *load name_of_file.plt*.

$f1(x) = 100/((a/x) - a + 1)$
$a = 1$
fit $f1(x)$ *"data.txt" using* 1:2 *via a*
plot "data.txt", $f1(x)$

An exemplary result of calculations performed in GUPLOT 5.0 on the basis of these commands is presented in Figure A8.

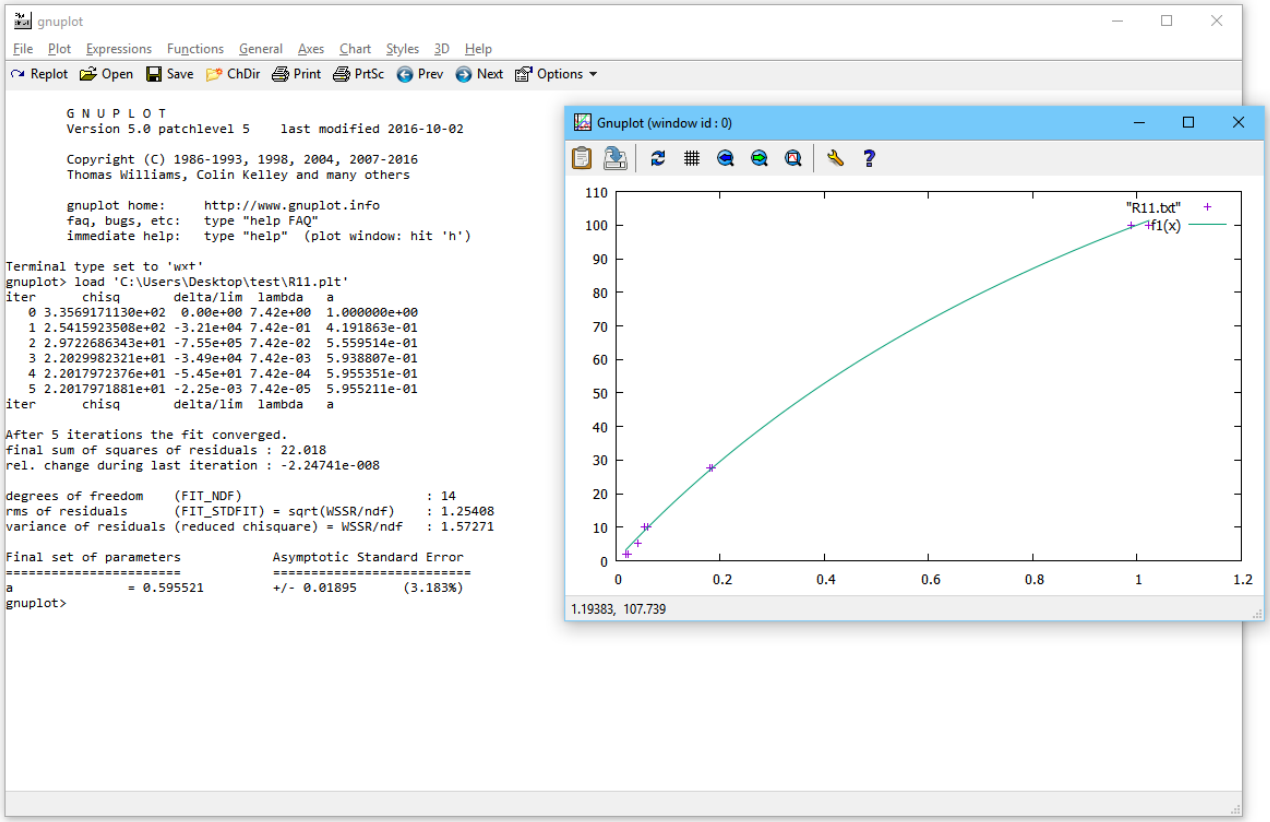

Figure A8. GNUPLOT 5.0 windows that show sample results of calculations that are based on the commands in GNUPLOT.

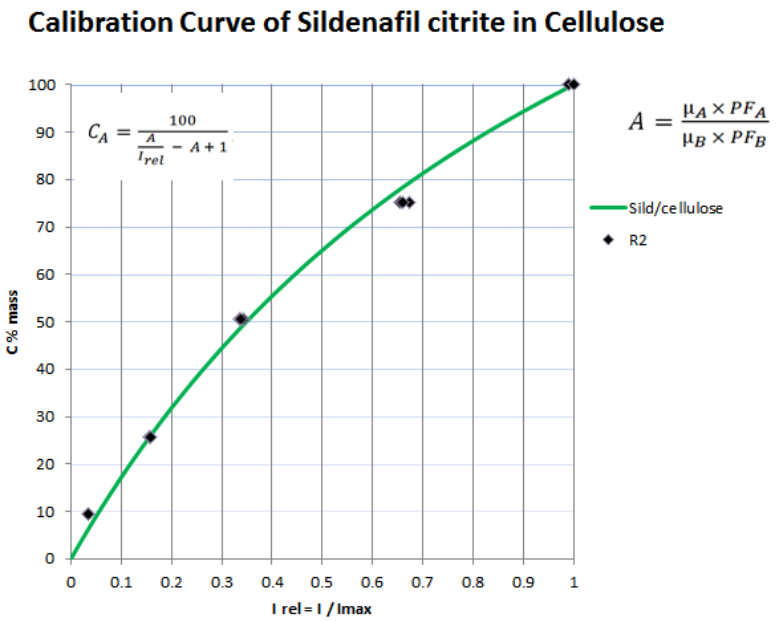

Figure A9. Another example of the calibration curve.

Appendix G

The error of estimating the arithmetic mean (standard deviation of the arithmetic mean) has been calculated as follows $s_{\overline{x}} = \sqrt{\frac{\sum_{i=1}^{n}(x_i - \overline{x})^2}{n(n-1)}}$.

Appendix H

Below, there are five plots (Figures A10–A14) with a graphical representation of the limit of detection and the limit of quantification for XRD measurements for different mixtures of compounds. QA descriptors stand for standard XRD measurements which can be used mainly for phase identification, whereas S-QTY stands for higher quality XRD measurements, which were used to check this semi-quantification method. Numerical data are in Table A3.

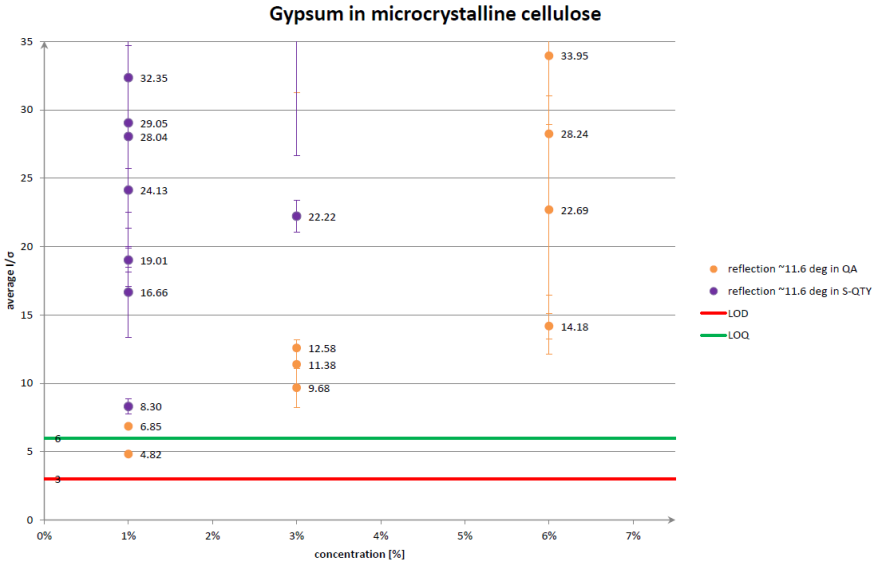

Figure A10. Graphical representation of the limit of detection (LOD) and limit of quantification (LOQ) for varied reflection in samples with varied concentrations of a two-phase mixture of calcium sulphate dihydrate and microcrystalline cellulose.

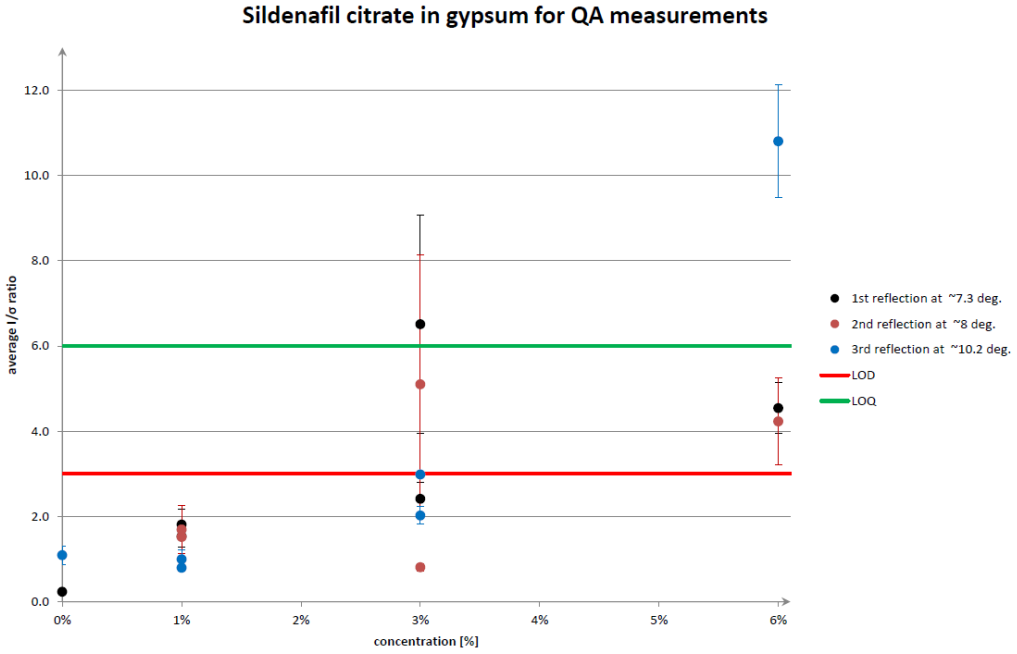

Figure A11. Graphical representation of the limit of detection (LOD) and limit of quantification (LOQ) for varied reflection in samples with varied concentrations of a two-phase mixture of sildenafil citrate and calcium sulphate dihydrate. Results are for the qualitative analyses (QA) settings of measurement.

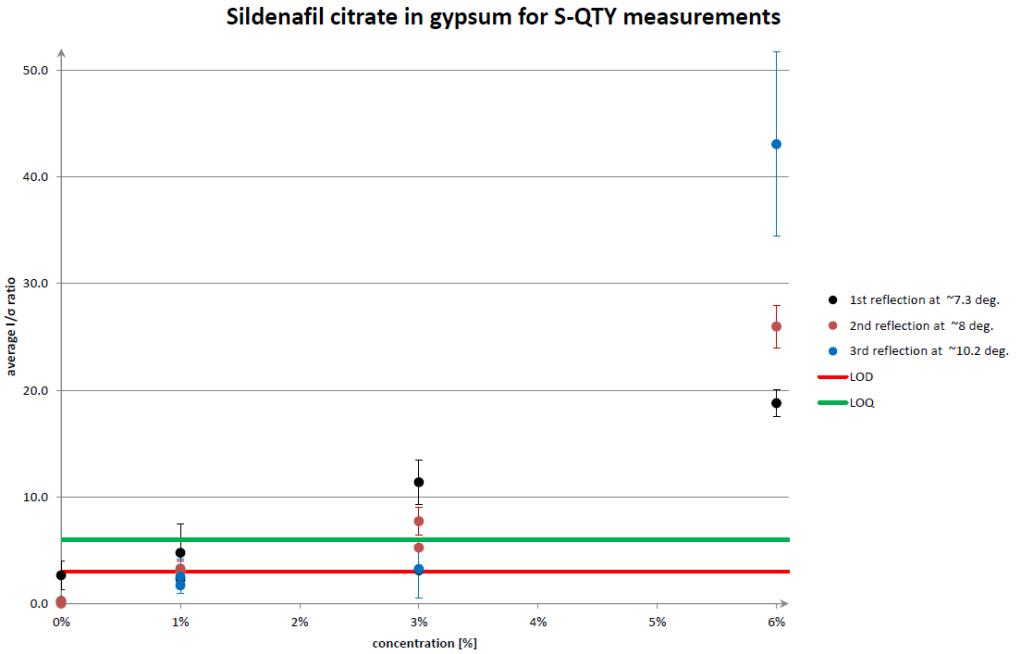

Figure A12. Graphical representation of the limit of detection (LOD) and limit of quantification (LOQ) for varied reflection in samples with varied concentrations of a two-phase mixture of sildenafil citrate and calcium sulphate dihydrate. Results are for the quantitative analyses (S-QTY) settings of measurement.

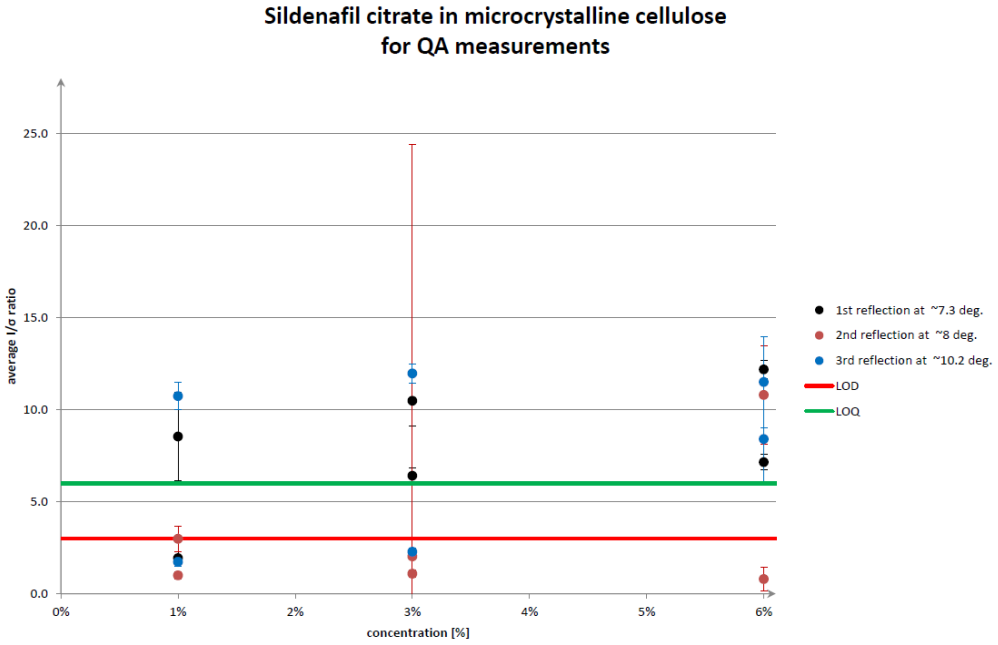

Figure A13. Graphical representation of the limit of detection (LOD) and limit of quantification (LOQ) for varied reflection in samples with varied concentrations of a two-phase mixture of sildenafil citrate and microcrystalline cellulose. Results are for the qualitative analyses (QA) settings of measurement.

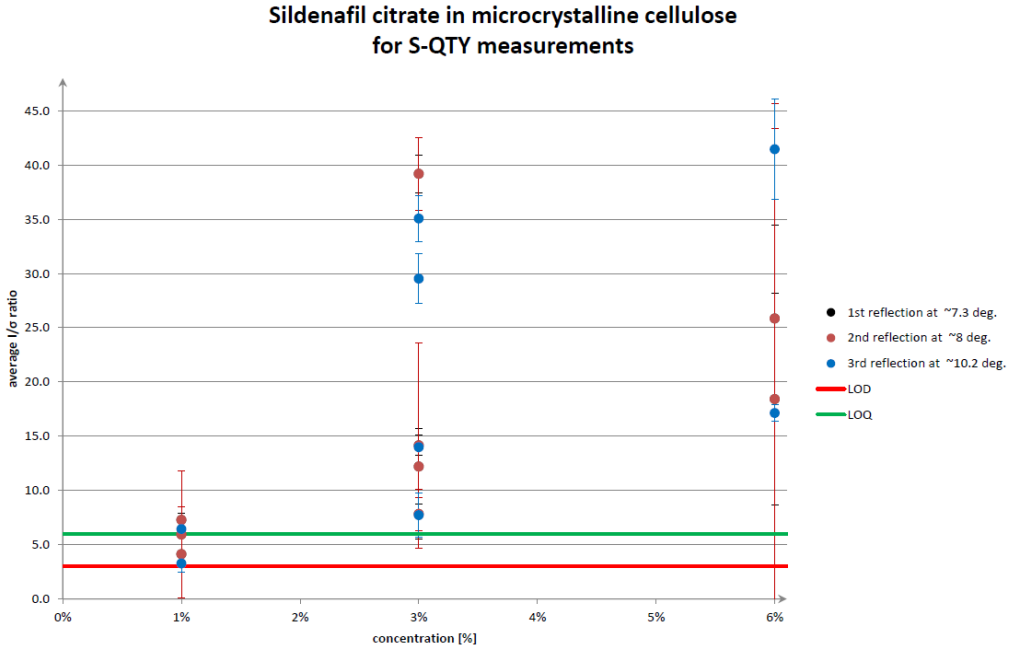

Figure A14. Graphical representation of the limit of detection (LOD) and limit of quantification (LOQ) for varied reflection in samples with varied concentrations of a two-phase mixture of sildenafil citrate and microcrystalline cellulose. Results are for the quantitative analyses (S-QTY) settings of measurement.

Table A3. Summary of LOD and LOQ.

Sildenafil Citrate in Gypsum			Sildenafil Citrate in Cellulose			Gypsum in Cellulose	Type of Measurement
Refl. 1	**Refl. 2**	**Refl. 3**	**Refl. 1**	**Refl. 2**	**Refl. 3**	**Refl. 1**	
3–6%	3–6%	6%	~3%	~6%	~6%	<1%	LOD (QA)
1%	1–3%	3%		<1%		<1%	LOD (S-QTY)
	~6%		3%	~6%		<1%	LOQ (QA)
	~3–6%			<3%		<1%	LOQ (S-QTY)

Appendix I

Data from the validation of LC-DAD and LC-QTOF-MS methods are below in Table A4.

Table A4. Intra-day and inter-day precision and accuracy data at a concentration range from 5 to 13 $\mu g \cdot mL^{-1}$ by the LC-DAD and LC-QTOF-MS methods.

Concentration Level [$\mu g \cdot mL^{-1}$]	Precision RSD [%]				Accuracy [%]			
	Intra-Day (n = 3)		Inter-Day (n = 9)		Intra-Day (n = 3)		Inter-Day (n = 9)	
	DAD	**MS**	**DAD**	**MS**	**DAD**	**MS**	**DAD**	**MS**
5	0.59	0.06	2.29	6.78	99.50	98.38	99.71	97.95
10	0.44	0.25	2.61	5.49	100.62	102.07	99.66	102.57
13	0.40	0.19	1.84	4.78	99.72	99.07	99.83	98.85

Appendix J

A modification of the measurement parameters can change the limit of quantification (LOQ) and limit of determination (LOD). Examples of visualizations that may help understand this are shown in Figures A15 and A16.

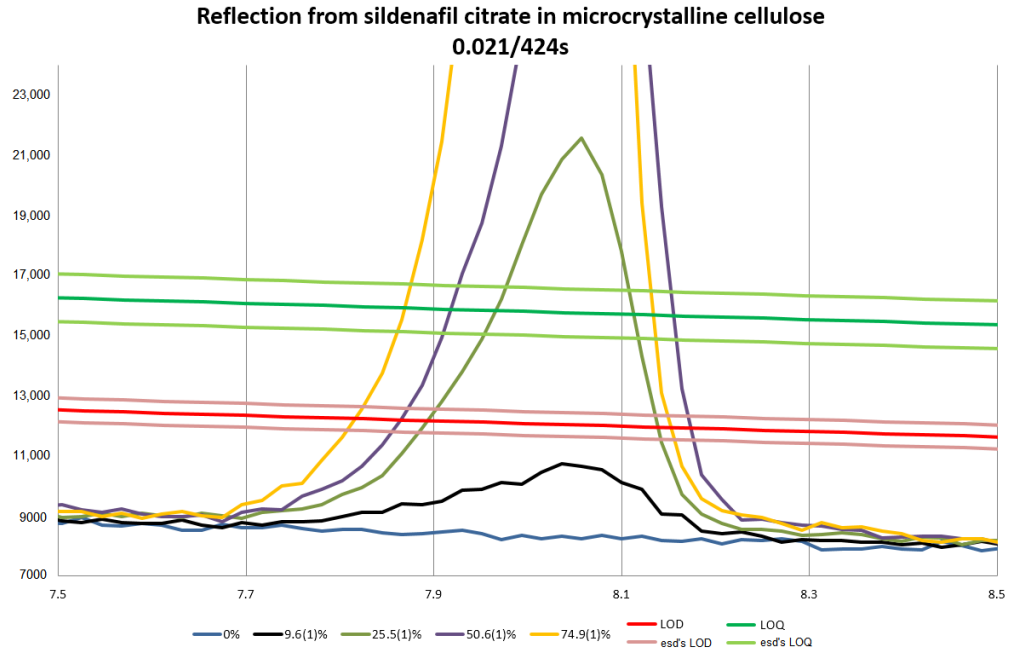

Figure A15. An example visualization of LOD and LOQ for reflection at $2\theta \approx 8.2°$ for sildenafil citrate in microcrystalline cellulose at different ratios. The measurement step size was 0.021°. The total time per step was 424 s.

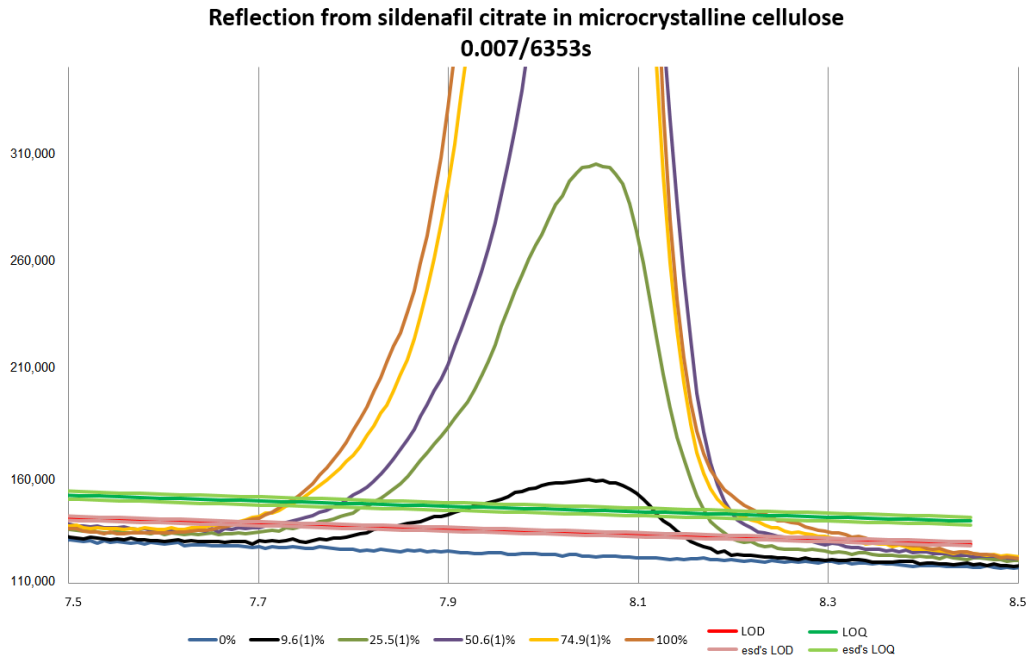

Figure A16. An example visualization of LOD and LOQ for reflection at $2\theta \approx 8.2^{\circ}$ for sildenafil citrate in microcrystalline cellulose at different ratios. The measurement step size was 0.007° and the total time per step was 6353 s.

Appendix K

In this section, the input data used in the article are collected. The relative intensities of reflections for sildenafil citrate are in Table A5, whereas for calcium sulphate dihydrate they are in Table A6. The mean value 0.993568 was the relative intensity of reflection calculated for calcium sulphate dihydrate (gypsum). The mean value 0.993568 was used.

Table A5. Relative intensities of reflections from sildenafil citrate were calculated from recorded diffractograms used as input data for concentration estimation.

Pure Sildenafil Citrate	F01	F02	C01	C02	C03
1.012759	0.07349	0.030196	0.086362	0.049646	0.088602
0.98554	0.07366	0.030026	0.087978	0.048908	0.088432
1.000851	0.07349	0.029487	0.086192	0.047491	0.088602
1.000851		0.031613	0.085058	0.044967	0.088375
1		0.030167	0.087156		0.088602
		0.031443	0.085682		

Table A6. Relative intensities of reflections from calcium sulphate dihydrate from recorded diffractograms were used as input data for concentration estimation.

C01	C02	C03
0.060665	0.060108	0.194202
0.059067	0.19425	0.233273
0.060593	0.19425	0.236008
	0.194106	0.233129
		0.234137

Appendix L

In this section powder diffraction data and patterns of sildenafil citrate, sildenafil citrate hemihydrate (or semihydrate) and sildenafil citrate monohydrate are collected (Figures A17 and A18). The powder diffraction patterns of sildenafil citrate and its modification under temperature have been presented in an article [40].

The ICDD 00-052-2420 pattern was obtained from the ICDD database, where the source is private communication at a conference or meeting. However, the same authors have published their results [39]. They reported the pattern for sildenafil citrate in a monoclinic system with the following unit cell dimensions: a = 26.98 Å, b = 11.95 Å, c = 16.68 Å and β = 106.96°, probably at room temperature. The atomic coordinates are not available. However, in the low-quality diffractogram in Figure 1 of the article [39], there are some extra reflections that are not present in the ICDD 00-052-2420 pattern. The pattern ICDD 00-052-2420 was also used in quite recent great work with the characterization of API in some tablets [43].

The structure CCDC FEDTEO/CCDC 264096/COD 2205085 is for sildenafil citrate monohydrate [37,44] in an orthorhombic system in the *Pbca* space group with unit cell dimensions of a = 24.002(4) Å, b = 10.9833(17) Å, c = 24.364(3) Å; Z = 8 at 173(2) K.

The structure CCDC KAJYIG/CCDC 1062242/COD 7223973 is for sildenafil citrate hemihydrate (sometimes called semihydrate) [38,45]. It crystallized at 120 K in the *Pbca* space group of the orthorhombic system with unit cell dimensions of a = 24.0290(10) Å, b = 10.9805(5) Å, c = 24.3497(10) Å; Z = 8. In this case, it is worth mentioning that some databases provide only *x*, *y*, *z* atomics coordinates without atomic site occupations and therefore information about structural factors is modified during crystallographic operations including structure refinement. As a consequence, the intensity and shape of reflections for calculated powder diffractograms also change with atomic site occupations (see Figure A18).

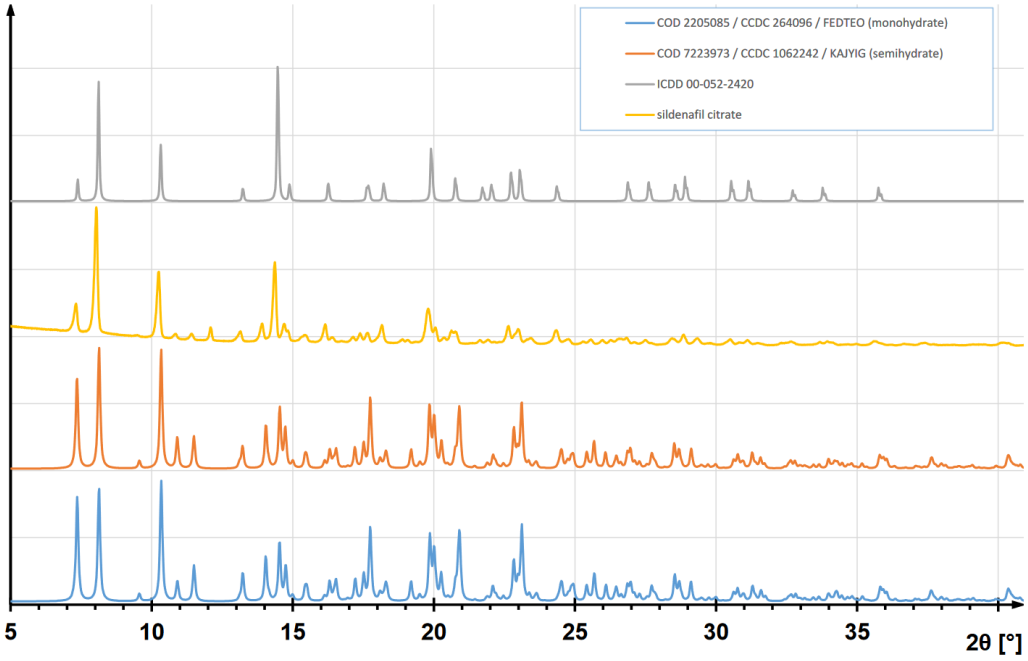

Figure A17. The diffractograms from the top are for the sildenafil citrate pattern ICDD 00-052-2420, sildenafil citrate measured in our laboratory, sildenafil citrate hemihydrate calculated from the crystal structure CCDC KAJYIG and sildenafil citrate monohydrate calculated from the crystal structure CCDC FEDTEO.

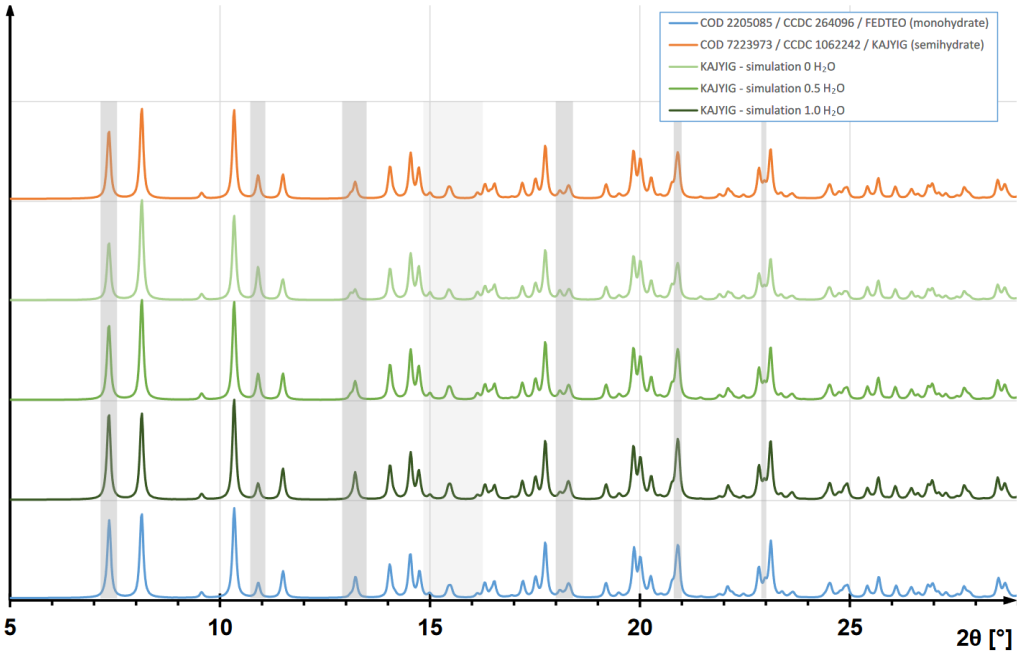

Figure A18. The diffractograms from the top are for sildenafil citrate hemihydrate calculated from the crystal structure CCDC KAJYIG, for the crystal structure CCDC KAJYIG with 0 occupations for atoms of water molecules, for the crystal structure CCDC KAJYIG (half occupations for atoms of water molecules—the original structure KAJYIG was not modified), for the crystal structure CCDC KAJYIG with full occupations for atoms of water molecules and for sildenafil citrate monohydrate calculated from the crystal structure CCDC FEDTEO.

References

1. Aldhous, P. Counterfeit pharmaceuticals: Murder by medicine. *Nature* **2005**, *434*, 132–137. [CrossRef]
2. Everts, S. Fake pharmaceuticals. Those fighting against counterfeit medicines face increasingly sophisticated adversaries. *Chem. Eng. News* **2010**, *88*, 27–29. [CrossRef]
3. Hanif, M.; Mobarak, M.R.; Ronan, A.; Rahman, D.; Donovan, J.J.; Bennish, M.L. Fatal renal failure caused by diethylene glycol in paracetamol elixir: The Bangladesh epidemic. *BMJ* **1995**, *311*, 88–91. [CrossRef]
4. Newton, P.N.; McGready, R.; Fernandez, F.; Green, M.D.; Sunjio, M.; Bruneton, C.; Phanouvong, S.; Millet, P.; Whitty, C.J.M.; Talisuna, A.O.; et al. Manslaughter by Fake Artesunate in Asia—Will Africa Be Next? *PLoS Med.* **2006**, *3*, e197. [CrossRef]
5. Newton, P.N.; Fernández, F.M.; Plançon, A.; Mildenhall, D.C.; Green, M.D.; Ziyong, L.; Christophel, E.M.; Phanouvong, S.; Howells, S.; McIntosh, E.; et al. A Collaborative Epidemiological Investigation into the Criminal Fake Artesunate Trade in South East Asia. *PLoS Med.* **2008**, *5*, e32. [CrossRef] [PubMed]
6. Dondorp, A.M.; Newton, P.N.; Mayxay, M.; Van Damme, W.; Smithuis, F.M.; Yeung, S.; Petit, A.; Lynam, A.J.; Johnson, A.; Hien, T.T.; et al. Fake antimalarials in Southeast Asia are a major impediment to malaria control: Multinational cross-sectional survey on the prevalence of fake antimalarials. *Trop. Med. Int. Health* **2004**, *9*, 1241–1246. [CrossRef]
7. World Health Organization. Available online: http://www.who.int/teams/regulation-prequalification/incidents-and-SF/background/definitions (accessed on 30 August 2023).
8. World Health Organization. Substandard and Falsified Medical Products. Available online: https://www.who.int/news-room/fact-sheets/detail/substandard-and-falsified-medical-products (accessed on 25 August 2023).
9. World Health Organization. *WHO Expert Committee on Specifications for Pharmaceutical Preparations, Fifty-Second Report*; WHO Technical Report Series, No. 1010; World Health Organization: Geneva, Switzerland, 2018. Available online: https://apps.who.int/iris/handle/10665/272452 (accessed on 30 August 2023).
10. Olliaro, E.; Olliaro, P.; Ho, C.W.L.; Ravinetto, R. Legal Uncertainty—The Gray Area around Substandard Medicines: Where Public Health Meets Law. *Am. J. Trop. Med. Hyg.* **2020**, *102*, 262–267. [CrossRef]
11. WHO. Recommendations for Health Authorities on Criteria for Risk Assessment and Prioritization of Cases: Executive Summary. Provisional Agenda Item 4A on Seventh Meeting of the Member State Mechanism on A/MSM/7/3 Substandard and Falsified Medical Products. 20 November 2018. Available online: https://apps.who.int/gb/SF/pdf_files/MSM7/A_MSM7_3-en.pdf (accessed on 30 August 2023).
12. World Health Organization. *WHO Global Surveillance and Monitoring System for Substandard and Falsified Medical Products*; World Health Organization: Geneva, Switzerland, 2017. Available online: https://apps.who.int/iris/handle/10665/326708 (accessed on 30 August 2023).

13. Deisingh, A.K. Pharmaceutical counterfeiting. *Analyst* **2005**, *130*, 271–279. [CrossRef]
14. Jackson, G.; Arver, S.; Banks, I.; Stecher, V.J. Counterfeit phosphodiesterase type 5 inhibitors pose significant safety risks. *Int. J. Clin. Pract.* **2010**, *64*, 497–504. [CrossRef]
15. Johnston, A.; Holt, D.W. Substandard drugs: A potential crisis for public health. *Br. J. Clin. Pharmacol.* **2014**, *78*, 218–243. [CrossRef] [PubMed]
16. Keizers, P.H.; Wiegard, A.; Venhuis, B.J. The quality of sildenafil active substance of illegal source. *J. Pharm. Biomed. Anal.* **2016**, *131*, 133–139. [CrossRef] [PubMed]
17. Maurin, J.K.; Pluciński, F.; Mazurek, A.P.; Fijałek, Z. The usefulness of simple X-ray powder diffraction analysis for counterfeit control—The Viagra® example. *J. Pharm. Biomed. Anal.* **2007**, *43*, 1514–1518. [CrossRef]
18. Venhuis, B.; Vredenbregt, M.; Kaun, N.; Maurin, J.; Fijałek, Z.; de Kaste, D. The identification of rimonabant polymorphs, sibutramine and analogues of both in counterfeit Acomplia bought on the internet. *J. Pharm. Biomed. Anal.* **2011**, *54*, 21–26. [CrossRef]
19. Sherma, J. Analysis of Counterfeit Drugs by Thin Layer Chromatography. *Acta Chromatogr.* **2007**, *19*, 5–20.
20. Neuberger, S.; Neusüß, C. Determination of counterfeit medicines by Raman spectroscopy: Systematic study based on a large set of model tablets. *J. Pharm. Biomed. Anal.* **2015**, *112*, 70–78. [CrossRef] [PubMed]
21. Rodionova, O.Y.; Houmøller, L.P.; Pomerantsev, A.L.; Geladi, P.; Burger, J.; Dorofeyev, V.L.; Arzamastsev, A.P. NIR spectrometry for counterfeit drug detection: A feasibility study. *Anal. Chim. Acta* **2005**, *549*, 151–158. [CrossRef]
22. Sacré, P.-Y.; Deconinck, E.; De Beer, T.; Courselle, P.; Vancauwenberghe, R.; Chiap, P.; Crommen, J.; De Beer, J.O. Comparison and combination of spectroscopic techniques for the detection of counterfeit medicines. *J. Pharm. Biomed. Anal.* **2010**, *53*, 445–453. [CrossRef] [PubMed]
23. de Veij, M.; Deneckere, A.; Vandenabeele, P.; de Kaste, D.; Moens, L. Detection of counterfeit Viagra® with Raman spectroscopy. *J. Pharm. Biomed. Anal.* **2008**, *46*, 303–309. [CrossRef] [PubMed]
24. Poplawska, M.; Blazewicz, A.; Bukowinska, K.; Fijalek, Z. Application of high-performance liquid chromatography with charged aerosol detection for universal quantitation of undeclared phosphodiesterase-5 inhibitors in herbal dietary supplements. *J. Pharm. Biomed. Anal.* **2013**, *84*, 232–243. [CrossRef] [PubMed]
25. Bruker AXS. *EVA 14, DIFFRACplus Basic Evaluation Package*; Bruker AXS: Karlsruhe, Germany, 2008.
26. Coelho, A. *TOPAS Academic*, Version 4.1; Coelho Software: Brisbane, Australia, 2007.
27. Wojdyr, M. Fityk: A general-purpose peak fitting program. *J. Appl. Crystallogr.* **2010**, *43*, 1126–1128. [CrossRef]
28. Johnson, Q.; Zhou, R.S. Checking and Estimating RIR Values, International Centre for Diffraction Data. *Adv. X-ray Anal.* **2000**, *42*, 287–296.
29. International Conference on Harmonization (ICH). Topic Q2 (R1): Validation of Analytical Procedures: Text and Methodology. Validation of Analytical Procedures: Text and methodology. 2005. Available online: http://www.ema.europa.eu/docs/en_GB/document_library/Scientific_guideline/2009/09/WC500002662.pdf (accessed on 21 August 2023).
30. JCPDS–International Centre for Diffraction Data®. *PDF-2/PDF-4 "Powder Diffraction File", 1997–2016*; JCPDS–International Centre for Diffraction Data®: Newtown Square, PA, USA, 2016.
31. Downs, R.T.; Hall-Wallace, M. The American mineralogist crystal structure database. *Am. Miner.* **2003**, *88*, 247–250.
32. Gražulis, S.; Chateigner, D.; Downs, R.T.; Yokochi, A.F.T.; Quirós, M.; Lutterotti, L.; Manakova, E.; Butkus, J.; Moeck, P.; Le Bail, A. Crystallography Open Database–An open-access collection of crystal structures. *J. Appl. Crystallogr.* **2009**, *42*, 726–729. [CrossRef]
33. Gražulis, S.; Daškevič, A.; Merkys, A.; Chateigner, D.; Lutterotti, L.; Quirós, M.; Serebryanaya, N.R.; Moeck, P.; Downs, R.T.; Le Bail, A. Crystallography Open Database (COD): An open-access collection of crystal structures and platform for world-wide collaboration. *Nucleic Acids Res.* **2012**, *40*, D420–D427. [CrossRef]
34. Gražulis, S.; Merkys, A.; Vaitkus, A.; Okulič-Kazarinas, M. Computing stoichiometric molecular composition from crystal structures. *J. Appl. Crystallogr.* **2015**, *48*, 85–91. [CrossRef]
35. Jenkins, R.; de Vries, J.L. *An Introduction to Powder Diffractometry*; N.V. Philips: Eindhoven, The Netherlands, 1977.
36. Brandt, C.G.; Kinneging, A.J. *X-ray Powder Diffraction. A Practical Guide to Quantitative Phase Analysis*; PANalytical B.V.: Almelo, The Netherlands, 2005.
37. Yathirajan, H.S.; Nagaraj, B.; Nagaraja, P.; Bolte, M. Sildenafil citrate monohydrate. *Acta Cryst. E* **2005**, *E61*, o489–o491. [CrossRef]
38. Abraham, A.; Apperley, D.C.; Byard, S.J.; Ilott, A.J.; Robbins, A.J.; Zorin, V.; Harris, R.K.; Hodgkinson, P. Characterising the role of water in sildenafil citrate by NMR crystallography. *CrystEngComm* **2016**, *18*, 1054–1063. [CrossRef]
39. Melnikov, P.; Corbi, P.P.; Cuin, A.; Cavicchioli, M.; Guimarães, W.R. Physicochemical Properties of Sildenafil Citrate (Viagra) and Sildenafil Base. *J. Pharm. Sci.* **2003**, *92*, 2140–2143. [CrossRef]
40. Ho, H.M.K.; Xiong, Z.; Wong, H.Y.; Buanz, A. The era of fake medicines: Investigating counterfeit medicinal products for erectile dysfunction disguised as herbal supplements. *Int. J. Pharm.* **2022**, *617*, 121592. [CrossRef]
41. Willson, A.J.C. *International Tables for Crystallography Volume C: Mathematical, Physical and Chemical Tables*; Kluwer Academic Publishers: Dordrecht, The Netherlands; Boston, MA, USA; London, UK, 1995.
42. El-Abadelah, M.M.; Sabri, S.S.; Khanfar, M.A.; Voelter, W.; Maichle-Mössmer, C. X-Ray Structure Analysis of iso-Sildenafil (iso-Viagra). *Z. Naturforsch. B* **1999**, *54*, 1323–1326. [CrossRef]
43. Jendrzejewska, I.; Goryczka, T.; Pietrasik, E.; Klimontko, J.; Jampilek, J. Identification of Sildenafil Compound in Selected Drugs Using X-ray Study and Thermal Analysis. *Molecules* **2023**, *28*, 2632. [CrossRef] [PubMed]

44. CCDC CSD Entry FEDTEO. Available online: https://www.ccdc.cam.ac.uk/structures/Search?Ccdcid=FEDTEO (accessed on 30 August 2023).
45. CCDC CSD Entry KAJYIG. Available online: https://dx.doi.org/10.5517/cc14nbw0 (accessed on 30 August 2023).